RSC Advances

REVIEW

View Article Online
View Journal | View Issue



Cite this: *RSC Adv.*, 2024, **14**, 20492

# Light-driven photocatalysis as an effective tool for degradation of antibiotics

Praveen P. Singh,[a] Geetika Pandey,[b] Yogesh Murti,[c] Jagriti Gairola,[de] Shriya Mahajan,[f] Harsimrat Kandhari,[g] Shraddha Tivari[h] and Vishal Srivastava *[h]

Received 9th May 2024
Accepted 22nd June 2024

DOI: 10.1039/d4ra03431g

rsc.li/rsc-advances

Antibiotic contamination has become a severe issue and a dangerous concern to the environment because of large release of antibiotic effluent into terrestrial and aquatic ecosystems. To try and solve these issues, a plethora of research on antibiotic withdrawal has been carried out. Recently photocatalysis has received tremendous attention due to its ability to remove antibiotics from aqueous solutions in a cost-effective and environmentally friendly manner with few drawbacks compared to traditional photocatalysts. Considerable attention has been focused on developing advanced visible light-driven photocatalysts in order to address these problems. This review provides an overview of recent developments in the field of photocatalytic degradation of antibiotics, including the doping of metals and non-metals into ultraviolet light-driven photocatalysts, the formation of new semiconductor photocatalysts, the advancement of heterojunction photocatalysts, and the building of surface plasmon resonance-enhanced photocatalytic systems.



## 1. Introduction

Since antibiotics have the ability to affect humans and natural ecosystems, as well as to cause pathogenic bacteria to acquire antibiotic resistance at microconcentrations, the issue of water contamination *via* antibiotic residues is of concern globally.[1] Treatment for infectious diseases and agricultural productivity[2–5] have significantly improved as a result of the widespread use of antibiotics. On the basis of pharmacological characteristics, antibiotics are mainly divided into aminoglycosides, sulfonamides (SAs), glycopeptides macrolides, β-lactams, quinolones and tetracyclines.[6] Antibiotics are more difficult to remove because of their strong chemical stability. The parent structure of various antibiotics, classification and their characteristics have been summarized in Table 1.

Pharmaceutical antibiotics usually get poorly absorbed and metabolised by humans as well as animals. The release of polluted water, faeces, and urine from the aforementioned contact spots along with an escalated concentration of antibiotic residues, poses possible risks to the ecosystem (Fig. 1).[17] Consequently, the advancement of an affordable and efficient antibiotic decontamination technique is required. Until lately a variety of strategies, including photoelectric Fenton, biological elimination, photocatalytic degradation, membrane filtering, and adsorption, have been used to remediate antibiotic wastewater contaminants.[18a–h] In the realm of environmental remediation, photocatalytic technology is widely employed to oxidise antibiotics into molecules that are easily biodegradable, less hazardous, and even harmless due to which it has received much concern from scientists.[18i,j] As we continue our work on photocatalyzed organic synthesis,[19,20] this article provides an overview of current developments in the state-of-the-art design and production of photocatalysts with visible light sensitivity for the photocatalytic degradation of wastewater containing antibiotics.

## 2. Methods for antibiotic degradation

There are now multiple techniques to remove antibiotic residues in water and wastewater before releasing them back into the environment. The primary approaches employed as of right now includes both long-standing methods and more contemporary ideas.[21–24] Unfortunately, substantial mineralization is either extremely difficult to attain or would take excessively prolonged. Because of their poor selectivity, these techniques can have the unintended consequence of killing non-target creatures that leads to unintended damages.[25,26] This approach also has significant operating and capital expenditures. When removing antibiotic residues from water,

[a]*Department of Chemistry, United College of Engineering & Research, Prayagraj, U.P.-211010, India. E-mail: ppsingh23@gmail.com*
[b]*Department of Physics, Faculty of Science, United University, Prayagraj-211012, India*
[c]*Institute of Pharmaceutical Research, GLA University, Mathura-281406, India*
[d]*School of Pharmacy, Graphic Era Hill University, Clement Town, Dehradun, 248002 Uttarakhand, India*
[e]*Department of Allied Sciences, Graphic Era (Deemed to be University) Clement Town, Dehradun, 248002 Uttarakhand, India*
[f]*Centre of Research Impact and Outcome, Chitkara University, Rajpura-140417, Punjab, India*
[g]*Chitkara Centre for Research and Development, Chitkara University, Himachal Pradesh-174103, India*
[h]*Department of Chemistry, CMP Degree College, University of Allahabad, Prayagraj, U.P.-211002, India. E-mail: vishalgreenchem@gmail.com*

Table 1 Classification and characteristics of antibiotics

| Antibiotic type | Representative | Function/hazard | Ref. |
|---|---|---|---|
| Tetracyclines | 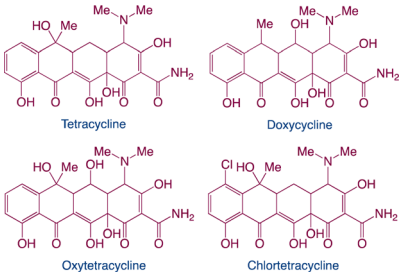  | Function: tetracyclines prevent livestock illness and promote growth<br>Hazard: result in significant persistence in the aquatic environment; increase the risk of certain infections, which may cause a negative effect on human; disturb the endocrine of aquatic species *etc.* | 7 |
| Sulfonamides | 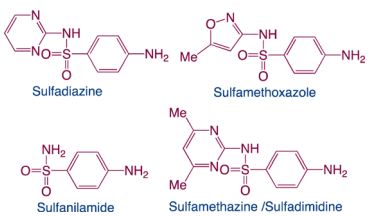  | Function: sulfonamides are used in human and veterinary medicine as antibacterial, especially in animal husbandry<br>Hazard: the toxicity of sulfonamides is not high to vertebrates. However, it can alter the function of microorganisms living in the environment. Additionally, the toxic effects of sulfonamides and other pollutants could show a synergism | 8 |
| Fluoroquinolones | 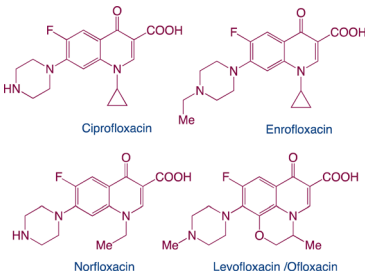  | Function: fluoroquinolones can kill bacteria or inhibit bacterial growth. Their primary function is to block the replication of DNA by inhibiting the function of DNA helicase. For humans, fluoroquinolones are an essential antibiotic for the treatment of severe invasive infections such as anthrax or plague<br>Hazard: promote resistance formation on microbial populations and induce toxic effects on aquatic organisms | 9 |
| Macrolides | 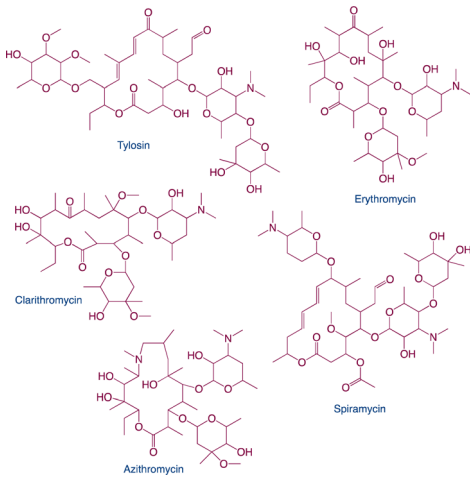  | Function: macrolides can inhibit bacterial protein synthesis and use to treat upper respiratory tract infections and soft-tissue infectionsHazard: it may cause liver damage using for a long time and result in macrolide resistance | 10 |
| β-lactams | 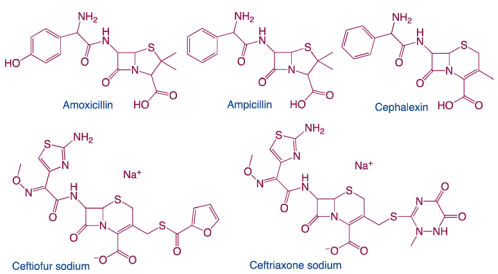  | Function: β-lactams are used to treat a variety of infections caused by susceptible bacteria, treat human genital tract infections, and serious infections. For animals, they can cure respiratory tract infections and intramammary disturbs<br>Hazard: it may cause an allergic reaction in sensitive person and influent plastid division in lower plants | 11 |
| Nitroimidazoles | | Function: nitroimidazoles have antiprotozoal and antibacterial activities as well as strong anti-anaerobic effects<br>Hazard: potential nephrotoxicity, carcinogenesis, and neurotoxicity in human | 12 |

Table 1 (*Contd.*)

| Antibiotic type | Representative | Function/hazard | Ref. |
|---|---|---|---|
| Glycopeptides |  Metronidazole Ornidazole Tinidazole 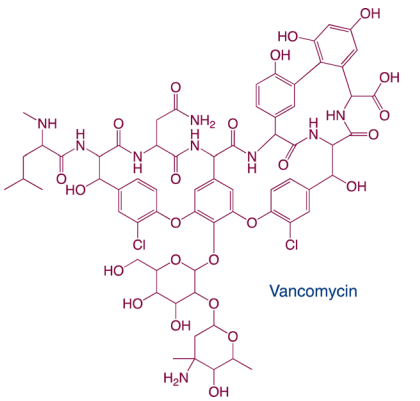 Vancomycin | Function: glycopeptides are commonly used to treat infections caused by streptococcus or enterococcus<br>Hazard: ototoxicity, nephrotoxicity, allergic reactions *etc.* | 13 |
| Aminoglycosides | 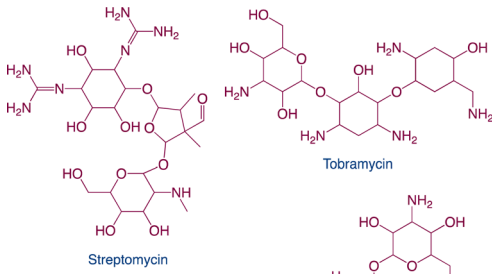 Streptomycin Tobramycin 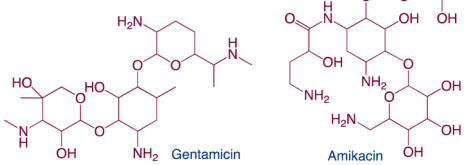 Gentamicin Amikacin | Function: aminoglycosides can promote the growth of animals<br>Hazard: high toxicity and nephrotoxicity in human | 14 |
| Chloramphenicol | 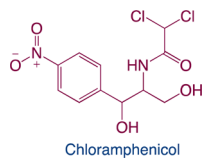 Chloramphenicol | Function: chloramphenicol is used for several infectious diseases such as flu bacillus infection<br>Hazard: may cause aplastic anemia and agranulocytosis | 15 |
| Lincomycin | 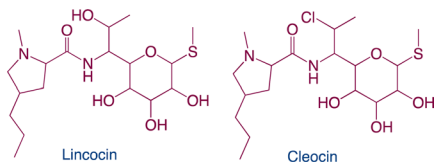 Lincocin Cleocin | Function: lincomycin is applied in food animals for the therapy of dysentery porcine proliferative enteropathies in pig *etc.*<br>Hazard: allergic reactions *etc.* | 16 |

a combination of chemical and physical degradation methods can greatly lower the toxicity of treated effluents. However, these techniques are expensive and complicated.[27]

Conversely, having a distinct advantages of photocatalysis, makes it a viable option for environmental remediation because of its (1) easily attainable reaction conditions (*i.e.*, almost ambient temperature and pressure), its ability to use air oxygen as a potent oxidant, and its ability to use solar radiation as an energy source; (2) the potential complete breakdown of organic pollutants into harmless inorganic molecules like carbon dioxide and water; and (3) its strong redox ability, low cost, lack of adsorption saturation, and long durability. As a result, photocatalysis has attracted attention from all around the world and been widely used in innovative methods of energy extraction and environmental control. Several methods[28–47] for antibiotic degradation have been reported incorporating materials, operating conditions and disadvantages of antibiotics.

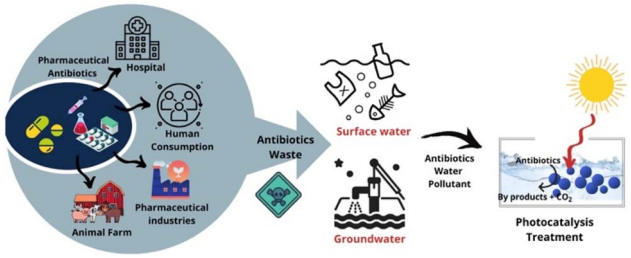


Fig. 1 Schematic representation of antibiotics consumption routes and impact on water bodies along with proposal of treating the same with solar energy-driven photocatalysis technique. Reproduced with permission from ref. 17. Copyright 2021 Elsevier Publishers.

## 3. General mechanism of photocatalytic antibiotics degradation

Techniques have been developed to treat contaminated water and waste water with organic pollutants. Fig. 2 depicts the mechanism of the photocatalytic degradation. An equivalent number of positively charged holes are produced in the valence band (VB) of a semiconductor when it is subjected to radiation with energy greater than its optical band gap. This is caused by excited electrons that are moved from the VB to the CB. When the potential of VB *vs.* NHE is more positive than $H_2O/OH^{\bullet}$(+2.72 V *vs.* NHE) or $OH^-/^{\bullet}OH$(+1.89 V *vs.* NHE) and the potential of CB *vs.* NHE is more negative than $O_2/^{\bullet}O_2^-$ (−0.33 V *vs.* NHE), the semiconductor will be able to generate $OH^{\bullet}$ and $^{\bullet}O_2^-$. After that, the photoinduced electrons and holes separate out and go to the semiconductor's surface, where redox reactions take place at the reactive site (Fig. 2).[21,48] The reaction mechanisms of semiconductor photocatalysis are typically expressed by the following equations:[49]

$$\text{semiconductor} + \text{light energy } (\lambda \geq E_g) \rightarrow \text{semiconductor } (e_{cb}^- + h_{vb}^+) \quad (1)$$

$$h_{vb}^+ + H_2O \rightarrow H^+ + {}^{\bullet}OH\ (H_2O/{}^{\bullet}OH| + 2.72\ \text{V } \textit{vs.}\ \text{NHE}) \quad (2)$$

$$h_{vb}^+ + OH^- \rightarrow {}^{\bullet}OH\ (OH^-/{}^{\bullet}OH| + 1.89\ \text{V } \textit{vs.}\ \text{NHE}) \quad (3)$$

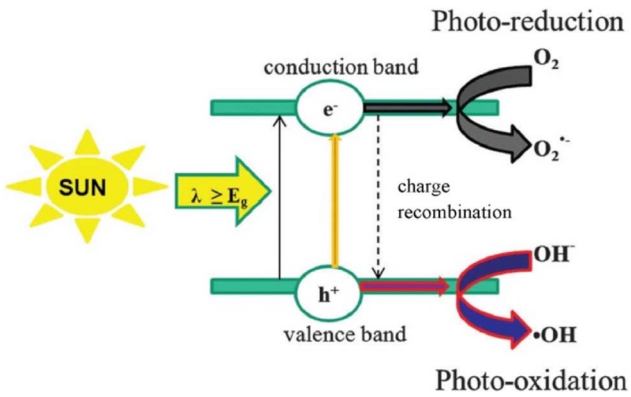


Fig. 2 General mechanism of the semiconductor photocatalytic degradation of organic pollutants. Reproduced with permission from ref. 21. Copyright 2020 Elsevier B.V. All rights reserved.

$$e_{cb}^- + O_2 \rightarrow {}^{\bullet}O_2^-(O_2/{}^{\bullet}O_2^-| - 0.33\ \text{V } \textit{vs.}\ \text{NHE}) \quad (4)$$

By these chemical processes solar energy can be directly converted and utilized. The consequences of photocatalytic activity are, however, lessened by restricted optical usage and the rapid annihilation of photoexcited electron–hole pairs. If photocatalysts satisfy the following requirements, they can overcome these deficiencies: (1) suitable spectral absorption range; (2) appropriate band energy structure for sufficient electron–hole pair separation and transport; and (3) sufficient active sites for adsorption or reaction.[50] To increase photocatalytic efficiency, it is imperative to meet the three previously mentioned requirements. Several attempts have been made to methodically design photocatalysts and enhance photocatalytic dynamics.

An acceptor is reduced by this excited electron, and donor molecules are oxidised by the acceptor's hole. The redox levels of the substrate[51–64] and the respective locations of the semiconductor's valence and conduction bands determine what happens to the excited electron and hole.

While considering photoabsorption capability and photocatalytic efficiency, optical bandgap ($E_g$) plays a crucial role in predicting the applicability and efficacy of a particular type of photocatalytic material. Polyfluorene co-polymers acting as photocatalysts[65,66] are classified as photonic and electrochemical bandgaps by Ghaedi *et al.*, who also proposed a method and criterion for bandgap measurement. Furthermore, they came to the conclusion that by keeping charges from recombining, the active holes' lifetime would increase and their ability to degrade antibiotics would be improved. This approach to the interfacial charge transfer from a distinct energy surface to a molecular continuous surface from solids[65,66] turned out to be highly effective in increasing the activity of photocatalysts under visible light.

Overall, the process of photocatalysis for the degradation of antibiotics can be broken down into five primary steps: (1) the antibiotics are transferred from the fluid phase to the surface; (2) they are adsorbed; (3) a reaction occurs in the adsorbed phase; (4) the products are desorption; and (5) the products are removed from the interface region.[67,68] However, when the electrons that had been excited to CB quickly recombine with the separated holes in the VB before producing free radicals, photocatalytic degradation suffers from the issue of electron–hole recombination in the photocatalyst.[68] Adoption of particular photocatalysts with a low CB–VB bandgap energy and photocatalyst modifications are proposed as solutions for these issues, however this depends on numerous variable alternatives, such as tailored experimental conditions.[69,70]

## 4. Synthesis techniques of nanostructured photocatalysts

Several synthesis techniques have been used as summarised in Fig. 3. It is noteworthy that the following characteristics are essential for an efficient photocatalyst: (a) robust absorption of visible and UV light (*i.e.*, a suitable bandgap value, typically less

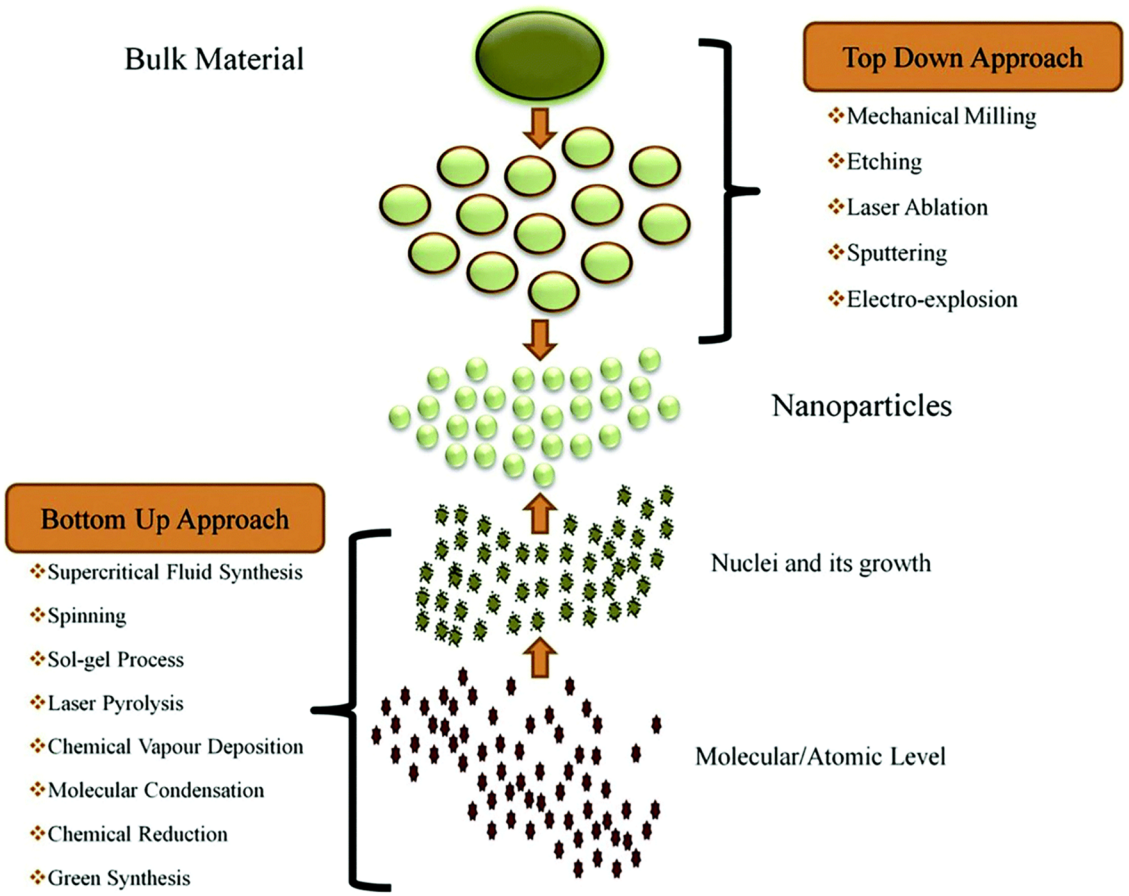


Fig. 3 Synthesis techniques of nanostructured photocatalysts. Reproduced with permission from ref. 75*a*. Copyright ©2019 Elsevier B.V. All rights reserved.

than 3.0 eV); (b) stability against photocorrosion in terms of temperature, chemical composition, and mechanical properties; (c) high efficiency in quantum conversion; (d) rapid generation and efficient transfer of photocarriers ($e^-$ and $h^+$); and (e) slow recombination rate of photogenerated charge carriers. Additionally, the nanopowder photocatalysts must be able to rapidly and easily recover from the solution while maintaining a sufficient level of reusability, or without noticeably losing effectiveness. To achieve the listed attributes, many tactics are now employed, such as tuning of particle

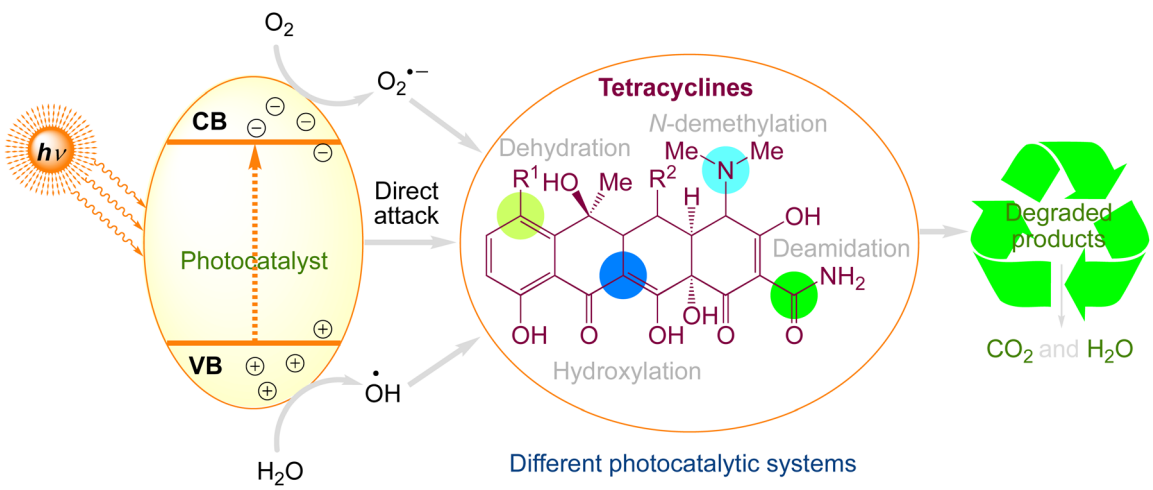


Fig. 4 The proposed photocatalytic degradation pathways of tetracyclines.

Table 2 Photocatalytic degradation of tetracyclines at different conditions

| Target antibiotic | Photocatalyst | Source of light | Optimum conditions: Initial concentration | Optimum conditions: Catalyst concentration | Degradation (%) | Ref. |
|---|---|---|---|---|---|---|
| Tetracycline | C dots modified $MoO_3$/g-$C_3N_4$ | Visible light | 20 mg $L^{-1}$ | 0.6 g $L^{-1}$ | 88.4% (90 min) | 88 |
| Tetracycline | g-$C_3N_4$/Hydroxyapatite | Simulated sunlight | 50 mg $L^{-1}$ | 1 g $L^{-1}$ | Almost 100% (15 min) | 89 |
| Tetracycline | β-$Bi_2O_3$/g-$C_3N_4$ core/shell nanocomposites | Visible light | 10 mg $L^{-1}$ | 0.5 g $L^{-1}$ | 80.2% (50 min) | 90 |
| Tetracycline | rGO/g-$C_3N_4$/$BiVO_4$ | Visible light | 35 mg $L^{-1}$ | 1 g $L^{-1}$ | 72.5% (150 min) | 91 |
| Tetracycline | C-doped $C_3N_4$/$Bi_{12}O_{17}Cl_2$ | Visible light | 20 mg $L^{-1}$ | 1 g $L^{-1}$ | 94.0% (60 min) | 92 |
| Tetracycline | $CeVO_4$/3D rGO aerogel/$BiVO_4$ | Visible light | 20 mg $L^{-1}$ | 0.5 g $L^{-1}$ | 100% (60 min) | 93 |
| Tetracycline | NGQDs-BiOI/$MnNb_2O_6$ | Visible light | 10 mg $L^{-1}$ | 0.5 g $L^{-1}$ | 87.2% (60 min) | 94 |
| Tetracycline | $TiO_2$/g-$C_3N_4$ | Simulated sunlight | 20 mg $L^{-1}$ | 1 g $L^{-1}$ | 100% (9 min) | 95 |
| Tetracycline | Amorphous $TiO_2$/mesoporous-rutile $TiO_2$ | UV light | 50 mg $L^{-1}$ | 0.5 g $L^{-1}$ | 81.1% (300 min) | 96 |
| Tetracycline | Magnetic $Fe_2O_3$ ultrathin nanosheets/ mesoporous black $TiO_2$ | Simulated sunlight | 10 mg $L^{-1}$ | 0.3 g $L^{-1}$ | 99.3% (50 min) | 97 |
| Tetracycline | $Bi_5FeTi_3O_{15}$ | Visible light | 5.0 mg $L^{-1}$ | 0.4 g $L^{-1}$ | 99.4% (60 min) | 98 |
| Tetracycline | $Bi_2WO_6$/$CuBi_2O_4$ | Visible light | 15 mg $L^{-1}$ | 0.5 g $L^{-1}$ | 91.0% (60 min) | 99 |
| Tetracycline | AgI/$BiVO_4$ | Visible light | 20 mg $L^{-1}$ | 3 g $L^{-1}$ | 94.9% (60 min) | 100 |
| Tetracycline | AgI/$WO_3$ | Visible light | 35 mg $L^{-1}$ | 3 g $L^{-1}$ | 75.0% (60 min) | 101 |
| Tetracycline | $Ag_3VO_4$/$WO_3$ | Visible light | 10 mg $L^{-1}$ | 0.5 g $L^{-1}$ | 71.2% (30 min) | 102 |
| Tetracycline | $Ag_3PO_4$/Zn–Al LDH | Simulated sunlight | 40 mg $L^{-1}$ | 1 g $L^{-1}$ | 96% (90 min) | 103 |
| Tetracycline | $FeNi_3/SiO_2$/CuS | UV light | 10 mg $L^{-1}$ | 5 g $L^{-1}$ | 96.7% (90 min) | 104 |
| Tetracycline | Fe-based MOFs | Visible light | 50 mg $L^{-1}$ | 0.5 g $L^{-1}$ | 96.6% (180 min) | 105 |
| Tetracycline | Pb/$MoO_4$ | Simulated sunlight | 20 mg $L^{-1}$ | 1 g $L^{-1}$ | 99.0% (120 min) | 106 |
| Tetracycline | Modified red mud | Visible light | 10 mg $L^{-1}$ | | 88.4% (80 min) | 107 |
| Tetracycline | $SnO_2$/g-$C_3N_4$ | Visible light | 30 mg $L^{-1}$ | 3 g $L^{-1}$ | 95.9% (120 min) | 108 |
| Tetracycline | RGO-CdTe | Visible light | 30 mg $L^{-1}$ | 3 g $L^{-1}$ | 83.6% (45 min) | 109 |
| Tetracycline | $Cu_2O$–$TiO_2$ | Visible light | 100 mg $L^{-1}$ | 1.5 g $L^{-1}$ | 100% (60 min) | 110 |
| Tetracycline | $Bi_2Sn_2O_7$/β-$Bi_2O_3$ | Visible light | 40 mg $L^{-1}$ | 2 g $L^{-1}$ | 95.5% (60 min) | 111 |
| Tetracycline | $MoS_2$/$TiO_2$ | Visible light | 10 mg $L^{-1}$ | 0.1 g $L^{-1}$ | 95.0% (100 min) | 112 |
| Tetracycline | $Bi_2Sn_2O_7$/$Bi_2MoO_6$ | Visible light | 35 mg $L^{-1}$ | 0.02 g $L^{-1}$ | 98.7% (100 min) | 113 |
| Tetracycline | $Ti_3C_2$@$TiO_2$ | Visible light | 20 mg $L^{-1}$ | | 90.0% (90 min) | 114 |
| Tetracycline | NiCo–S@CN | Solar light | 100 mg $L^{-1}$ | 2 g $L^{-1}$ | 99.0% (60 min) | 115*a* |
| Tetracycline | $Bi_2Sn_2O_7$/$Bi_2MoO_6$ | Visible light | 20 mg $L^{-1}$ | 0.035 g $L^{-1}$ | 98.7% (100 min) | 115*b* |
| Tetracycline | $Bi_2WO_6$/$Ta_3N_5$ | Visible light | 20 mg $L^{-1}$ | 0.04 g $L^{-1}$ | 86.7% (120 min) | 115*c* |
| Tetracycline | Ag/$Ag_2S$/$Bi_2MoO_6$ | Visible light | 20 mg $L^{-1}$ | 0.03 g $L^{-1}$ | 87.3% (120 min) | 115*d* |
| Oxytetracycline | Au–CuS–$TiO_2$ nanobelts | Simulated sunlight | 5.0 mg $L^{-1}$ | 0.114 $cm^2$ $ml^{-1}$ | 96.0% (60 min) | 116 |
| Oxytetracycline | N–$TiO_2$/graphene | UV light | 30 mg $L^{-1}$ | | 63.0% (160 min) | 117 |
| Oxytetracycline | $Ag_3PO_4$/$TiO_2$/$MoS_2$ | Visible light | 5 mg $L^{-1}$ | 0.5 g $L^{-1}$ | 90.0% | 118 |
| Oxytetracycline | Ti-MCM-41 | UV light | 50 mg $L^{-1}$ | 1 g $L^{-1}$ | 92.0% (180 min) | 119 |
| Oxytetracycline | g-$C_3N_4$ | Visible light | 20 mg $L^{-1}$ | 0.3 g $L^{-1}$ | 79.3% (60 min) | 120 |
| Oxytetracycline | $Fe_{2.8}Ce_{0.2}O_4$/GO | Visible light | 30 mg $L^{-1}$ | 0.8 g $L^{-1}$ | 82.0% (120 min) | 121 |
| Oxytetracycline | Rhombohedral corundum-type $In_2O_3$ | UV light | 10 mg $L^{-1}$ | 1 g $L^{-1}$ | 89.5% (120 min) | 122 |
| Oxytetracycline | $SnO_2$/BiOI | Visible light | 10 mg $L^{-1}$ | 1 g $L^{-1}$ | 94.6% (90 min) | 123 |
| Oxytetracycline | MU-0.15 | Simulated sunlight | 20 mg $L^{-1}$ | 0.5 g $L^{-1}$ | 86.6% (120 min) | 124 |
| Oxytetracycline | CoFe@NSC-1000 | Visible light | 50 mg $L^{-1}$ | 0.3 g $L^{-1}$ | 82.7% (150 min) | 125 |
| Oxytetracycline | $Fe_3O_4$/rGO/Co-doped ZnO/g-$C_3N_4$ | Visible light | 30 mg $L^{-1}$ | 0.16 g $L^{-1}$ | 82.0% (70 min) | 126 |
| Oxytetracycline | BiOI/$NH_2$-MIL125(Ti) | Visible light | 10 mg $L^{-1}$ | 0.5 g $L^{-1}$ | 96.2% (60 min) | 127 |
| Oxytetracycline | $MnFe_2O_4$/g-$C_3N_4$ | Visible light | 10 mg $L^{-1}$ | | 80.5% (10 min) | 128 |
| Oxytetracycline | MIL-100(Fe) | Visible light | 25 mg $L^{-1}$ | 0.05 g $L^{-1}$ | 99.0% (240 min) | 129 |
| Oxytetracycline | Ag/$BiVO_4$/GO | Visible light | 40 mg $L^{-1}$ | 0.4 g $L^{-1}$ | 90.43% (70 min) | 130 |
| Oxytetracycline | $TiO_2$ | Visible light | 10 mg $L^{-1}$ | 0.5 g $L^{-1}$ | 95.0% (180 min) | 131 |
| Oxytetracycline | $MnFe_2O_4$/g-$C_3N_4$ | Visible light | 10 mg $L^{-1}$ | | 90.0% (1 min) | 132 |
| Doxycycline | $SnO_2$/BiOI | Visible light | 10 mg $L^{-1}$ | 1 g $L^{-1}$ | 90.0% (60 min) | 133 |
| Doxycycline | Ag/AgCl/$CdMoO_4$ | UV light | 10 mg $L^{-1}$ | | 82.4% (60 min) | 134 |
| Doxycycline | α-$Bi_2O_3$/g-$C_3N_4$ + $H_2O_2$ | Visible light | 25 mg $L^{-1}$ | 0.01 g $L^{-1}$ | 79.0% (30 min) | 135 |
| Doxycycline | $TiO_2$-MCM-41 | UV light | 10 mg $L^{-1}$ | 0.15 g $L^{-1}$ | 85.0% (60 min) | 136 |
| Doxycycline | $In_2O_3$/g-$C_3N_4$ | | 10 mg $L^{-1}$ | | 99.3% (60 min) | 137 |

Table 2 (*Contd.*)

| Target antibiotic | Photocatalyst | Source of light | Optimum conditions: Initial concentration | Optimum conditions: Catalyst concentration | Degradation (%) | Ref. |
|---|---|---|---|---|---|---|
| | | Simulated sunlight | | | | |
| Doxycycline | $Cu_2O/SrBi_4Ti_4O_{15}$ | Visible light | 40 mg $L^{-1}$ | | 92.2% (60 min) | 138 |
| Chlorotetracycline | N–$TiO_2$/graphene | UV light | 30 mg $L^{-1}$ | | 54.0% (160 min) | 139 |
| Chlorotetracycline | $Bi_2O_3$/MIL101(Fe) | Visible light | 20 mg $L^{-1}$ | 0.3 g $L^{-1}$ | 88.2% (120 min) | 140 |

dimensions, morphology, and size. Moreover, different photocatalyst compositions result in heterojunctions, composites, core–shell structures, element substitutions, intercalation compounds, and plasmon sensitization.[51,71–75]

## 5. Photocatalytic degradation of different antibiotics

### 5.1. Photocatalytic degradation of tetracyclines

Tetracycline is a broad-spectrum antibiotic that is commonly used to treat a wide range of illnesses. Because of its high efficacy and low cost, it is regarded as the second most frequently used antibiotic in human activities and livestock breeding.[75–78] On the other hand, prolonged and excessive TC usage pollutes the environment and is a major social concern.[79] Tetracycline has been removed using a variety of methods, such as adsorption,[80] ion exchange,[81] membrane filtering,[82] biological processes,[83] electrolysis,[84] ozonation,[85] advanced oxidation processes,[86] and photocatalysis.[87] The most efficient, affordable, simple to implement, and environmentally benign of these processes are thought to be the photocatalysis and advanced oxidation processes. Generating charges such as holes, hydroxyl radicals, electrons, and superoxide anion radicals efficiently is essential to the photocatalysis process. Again, the exciton creation and its subsequent dissociation into photo-induced electrons and holes are prerequisites for the production of hydroxyl radical and superoxide anion radical.

Tetracyclines are generally used worldwide. They have four linked rings with several ionizable functional groups. The most widely used tetracyclines are oxytetracycline, tetracycline, and chlortetracycline. The degradation mechanisms of tetracyclines are more intricate because of their complex molecular structure.[77] Tetracycline degradation processes under various photocatalytic systems are summarised in Fig. 4. Tetracyclines are commonly degraded *via* four different processes: hydroxylation, deamidation, *N*-demethylation, and dehydration. Table 2 comprises a summary of the information regarding the photocatalytic degradation of tetracyclines using various photocatalysts.

### 5.2. Photocatalytic degradation of sulfonamides

Sulfonamides are a class of synthetic pharmaceuticals that emerged in 1906 and contain the sulfonamide chemical group. Since 1940, more than 150 of these agents have been utilised as antimicrobials, making them the most commonly used antibiotics in the field of medicine with good hydrophilicity.[141,142]

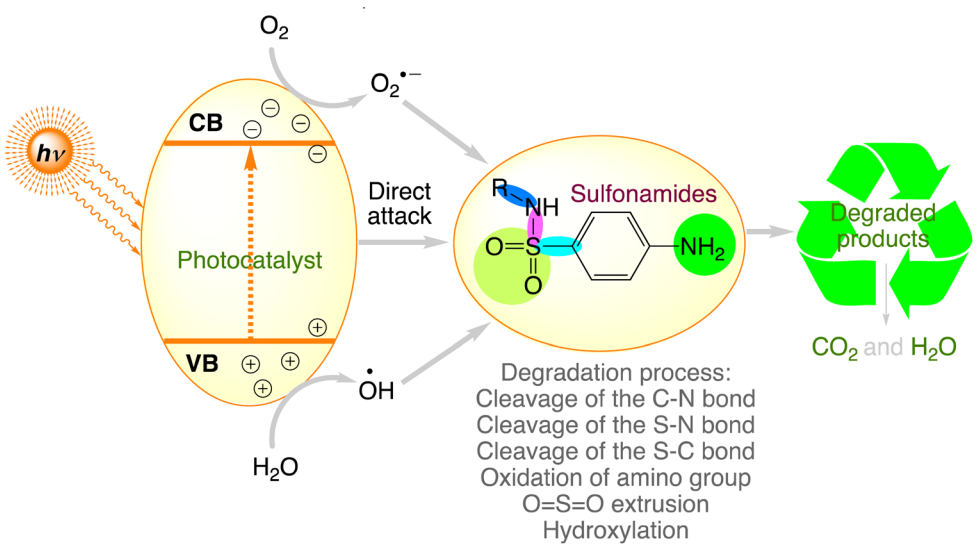


Fig. 5 The proposed photocatalytic degradation pathways of sulfonamides.

Table 3 Photocatalytic degradation of sulfonamides at different conditions

| | | | Optimum conditions | | | |
|---|---|---|---|---|---|---|
| Target antibiotic | Photocatalyst | Source of light | Initial concentration | Catalyst concentration | Degradation (%) | Ref. |
| Sulfamethoxazole | Doped metals (Na, K, Ca, Mg) on g-$C_3N_4$ | Visible light | 5.0 mg $L^{-1}$ | 0.05 g $L^{-1}$ | g-CN–K > g-CN–Na > g-CN–Mg > g-CN–Ca > g-CN | 144 |
| Sulfamethoxazole | Ag–P co-doped-g-$C_3N_4$ | Visible light | 5.0 mg $L^{-1}$ | 1.0 g $L^{-1}$ | 99% (30 min) | 145 |
| Sulfamethoxazole | Ag/P-g-$C_3N_4$ | Visible light | 0.1 mg $L^{-1}$ | 0.1 g $L^{-1}$ | 100% (20 min) | 146 |
| Sulfamethoxazole | Ag/g-$C_3N_4$/$Bi_3TaO_7$ | Visible light | 5.0 mg $L^{-1}$ | 0.5 g $L^{-1}$ | 98% (25 min) | 147 |
| Sulfamethoxazole | rGO/$WO_3$ | Visible light | 10.0 mg $L^{-1}$ | 2.0 g $L^{-1}$ | 98.0% (180 min) | 148 |
| Sulfamethoxazole | $Ag_3PO_4$/N-doped rGO | Visible light | 20.0 mg $L^{-1}$ | 0.2 g $L^{-1}$ | 93.8% (60 min) | 149 |
| Sulfamethoxazole | $TiO_2$-rGO | Simulated sunlight | 0.10 mg $L^{-1}$ | 0.1 g $L^{-1}$ | 87.0 ± 4% (60 min) | 150 |
| Sulfamethoxazole | $TiO_2$ supported on reed straw biochar | UV light | 10.0 mg $L^{-1}$ | 1.25 g $L^{-1}$ | 91.3% (180 min) | 151 |
| Sulfamethoxazole | W Modified $TiO_2$ | Simulated sunlight | 1.0 mg $L^{-1}$ | 0.25 g $L^{-1}$ | 100% (90 min) | 152 |
| Sulfamethoxazole | F–Pd co-doped-$TiO_2$ | Simulated sunlight | 30.0 mg $L^{-1}$ | 1.0 g $L^{-1}$ | 94.2% (20 min) | 153 |
| Sulfamethoxazole | p(HEA/NMMA)-CuS | UV light | 50.0 mg $L^{-1}$ | 2.0 g $L^{-1}$ | 95.9% (24 h) | 154 |
| Sulfamethoxazole | ZnO/fluoride ions | UV light | 250.0 mg $L^{-1}$ | 1.5 g $L^{-1}$ | 97.0% (30 min) | 155 |
| Sulfamethoxazole | Mn-$WO_3$ | LED light | 3.25 mg $L^{-1}$ | 2.3 g $L^{-1}$ | 100% (70 min) | 156 |
| Sulfamethoxazole | Co–CuS@$TiO_2$ | Solar light | 5.0 mg $L^{-1}$ | 1.0 g $L^{-1}$ | 100% (120 min) | 157 |
| Sulfamethoxazole | ZnO/$ZnIn_2S_4$ | Visible light | 2.5 mg $L^{-1}$ | 0.20 g $L^{-1}$ | 74.9% (6.5 h) | 158 |
| Sulfamethoxazole | $TiO_2$-based materials | Sunlight or LED | 10.0 mg $L^{-1}$ | | 90.0% (30 min) | 159 |
| Sulfamethoxazole | $TiO_2$/BC | UV light | 30.0 mg $L^{-1}$ | 0.02 g $L^{-1}$ | 89.0% (60 min) | 160 |
| Sulfamethoxazole | PAN-$TiO_2$ and PAN-rGTi | Solar light | 5.0 mg $L^{-1}$ | | 100% (120 min) | 161 |
| Sulfamethoxazole | $Fe_2O_3$/g-$C_3N_4$ | Visible light | 10.0 mg $L^{-1}$ | 0.3 g $L^{-1}$ | 99.2% (30 min) | 162 |
| Sulfamethoxazole | P–$TiO_2$/g-$C_3N_4$ | Visible light | 10.0 mg $L^{-1}$ | 0.7 g $L^{-1}$ | 99.0% (90 min) | 163 |
| Sulfamethoxazole | $TiO_2$@$Fe_2O_3$@g-$C_3N_4$ (MFTC) | Solar light | 10.0 mg $L^{-1}$ | 0.5 g $L^{-1}$ | 96.8% (120 min) | 164 |
| Sulfamethoxazole | Pd–$BiVO_4$ | Visible light | 10 mg $L^{-1}$ | | 98.8% (210 min) | 165 |
| Sulfamethoxazole | CoP/BVO | Simulated sunlight | 500 mg $L^{-1}$ | 1.0 g $L^{-1}$ | 89.0% (180 min) | 166 |
| Sulfamethoxazole | $MoS_2$@$CoS_2$ | Visible light | 20.0 mg $L^{-1}$ | | 95.0% (80 min) | 167 |
| Sulfamethoxazole | $ZrFe_2O_4$@ZIF-8 | Visible light | 5.0 mg $L^{-1}$ | 0.02 g $L^{-1}$ | 100% (180 min) | 168 |
| Sulfamethoxazole | CN/$N_2$PG-0.02 | Simulated sunlight | 10 mg $L^{-1}$ | | 90.0% (120 min) | 169 |
| Sulfamethoxazole | g-$C_3N_4$/GSBC | Visible light | 10.0 mg $L^{-1}$ | | 87.2% (90 min) | 170 |
| Sulfamethoxazole | Pt/$PtO_x$/$BiVO_4$ | Visible light | 10.0 mg $L^{-1}$ | 0.5 g $L^{-1}$ | 99.0% (150 min) | 171 |
| Sulfamethoxazole | Fe–Co/γ-$Al_2O_3$ | UV light | 10 mg $L^{-1}$ | 1.0 g $L^{-1}$ | 98.0% (60 min) | 172 |
| Sulfamethoxazole | Sulfur-doped-$Bi_2O_3$/$MnO_2$ (S-BOMO) | Visible light | 5.0 mg $L^{-1}$ | 0.5 g $L^{-1}$ | 86.0% (240 min) | 173 |
| Sulfamethoxazole | $Ag_3PO_4$ | UV light | 20.0 mg $L^{-1}$ | | 99.9% (60 min) | 174 |
| Sulfamethoxazole | Cd doped γ-$Bi_2MoO_6$ (Cd-BMO) | Visible light | 5.0 mg $L^{-1}$ | 0.05 g $L^{-1}$ | 97.9% (210 min) | 175 |
| Sulfamethoxazole | $AgNbO_3$ | Visible light | 10.0 mg $L^{-1}$ | 0.5 g $L^{-1}$ | 98.0% (8 h) | 176 |
| Sulfamethoxazole | Fc@rGO-ZnO | UV light | 10 mg $L^{-1}$ | | 95.0% (180 min) | 177 |
| Sulfamethoxazole | $CoFe_2O_4$/PMS | UV light | 10 mg $L^{-1}$ | 0.1 g $L^{-1}$/0.4 g $L^{-1}$ | 91.0% (10 min) | 178 |
| Sulfamethazine | g-$C_3N_4$ | Visible light | 10.0 mg $L^{-1}$ | 0.5 g $L^{-1}$ | 95.0% (24 h) | 179 |
| Sulfamethazine | g-$C_3N_4$ | Visible light | 10.0 mg $L^{-1}$ | 1.0 g $L^{-1}$ | 97.0% (60 min) | 180 |
| Sulfamethazine | g-$C_3N_4$ | Visible light | 30.0 mg $L^{-1}$ | 0.5 g $L^{-1}$ | 99.7% (60 min) | 181 |
| Sulfamethazine | C Doping g-$C_3N_4$ | Visible light | 10.0 mg $L^{-1}$ | 1.0 g $L^{-1}$ | 98.0% (60 min) | 182 |
| Sulfamethazine | 2D/1D g-$C_3N_4$/TNTs | Visible light | 5.0 mg $L^{-1}$ | 0.2 g $L^{-1}$ | 100% (5 h) | 183 |
| Sulfamethazine | $TiO_2$ | UV light | 20.0 mg $L^{-1}$ | 0.5 g $L^{-1}$ | 61.0% (120 min) | 184 |
| Sulfamethazine | AgI/$Bi_4V_2O_{11}$ | Visible light | 10.0 mg $L^{-1}$ | 0.1 g $L^{-1}$ | 91.5% (60 min) | 185 |
| Sulfamethazine | $Bi_2WO_6$/RGO | Simulated sunlight | 10.0 mg $L^{-1}$ | | 57.6% (8 h) | 186 |
| Sulfamethazine | Graphene aerogel/$Bi_2WO_6$ | Simulated sunlight | 10.0 mg $L^{-1}$ | | 55.8% (120 min) | 187 |
| Sulfamethazine | $W_{10}O_{32}^{4-}$ | Visible light | 13.9 mg $L^{-1}$ | 0.33 g $L^{-1}$ | 85.0% (4 h) | 188 |
| Sulfamethazine | g-$C_3N_4$/Cu, N–$TiO_2$ | | 10 mg $L^{-1}$ | | 95.8% (240 min) | 189 |

Table 3 (*Contd.*)

| Target antibiotic | Photocatalyst | Source of light | Optimum conditions: Initial concentration | Optimum conditions: Catalyst concentration | Degradation (%) | Ref. |
|---|---|---|---|---|---|---|
| | | Simulated sunlight | | | | |
| Sulfamethazine | $Cu–Cu_xO/TiO_2$ | Visible light | 10 mg $L^{-1}$ | | 98.2% (60 min) | 190 |
| Sulfamethazine | $PhC_2Cu/Ag/Ag_2MoO_4$ (PAM) | Visible light | 10.0 mg $L^{-1}$ | 0.4 g $L^{-1}$ | 97.7% (20 min) | 191 |
| Sulfamethazine | G-CDs | Simulated sunlight | 10.0 mg $L^{-1}$ | | 94.0% (75 min) | 192 |
| Sulfanilamide | $WO_3/Ag$ | Visible light | 10.0 mg $L^{-1}$ | 0.5 g $L^{-1}$ | 96.2% (5 h) | 193 |
| Sulfanilamide | $Ag/ZnFe_2O_4/Ag/BiTa_{1-x}V_xO_4$ | Visible light | 10.0 mg $L^{-1}$ | 1.0 g $L^{-1}$ | 100% (6 h) | 194 |
| Sulfanilamide | Mo–BiOBr | Visible light | 10.0 mg $L^{-1}$ | 0.3 g $L^{-1}$ | 48.3% (80 min) | 195 |
| Sulfadiazine | BiOCl–Au–CdS | Simulated sunlight | 20.0 mg $L^{-1}$ | 1.0 g $L^{-1}$ | 100% (240 min) | 196 |
| Sulfadiazine | $Cu_2O/Bi/Bi_2MoO_6$ | Visible light | 10.0 mg $L^{-1}$ | | 98.6% (100 min) | 197 |
| Sulfadiazine | Porous g-$C_3N_4$ with C vacancies | Visible light | 5.0 mg $L^{-1}$ | 0.02 g $L^{-1}$ | 100% (20 min) | 198 |
| Sulfadiazine | $NSFe–TiO_2$ | UV light | 20.0 mg $L^{-1}$ | 0.01 g $L^{-1}$ | 90.0% (120 min) | 199 |
| Sulfadiazine | $Bi_2O_3–TiO_2$/PAC | Visible light | 20.0 mg $L^{-1}$ | 0.2 g $L^{-1}$ | 72.0% (30 min) | 200 |
| Sulfadiazine | $TiO_2$/ZEO | UV light | 10.0 mg $L^{-1}$ | 1.0 g $L^{-1}$ | 90.0% (120 min) | 201 |
| Sulfadiazine | Degussa P25 $TiO_2$ | Visible light | 10.0 mg $L^{-1}$ | 1.0 g $L^{-1}$ | 99.0% (60 min) | 202 |
| Sulfadiazine | C, $N–TiO_2$@C | Visible light | 20.0 mg $L^{-1}$ | 1.0 g $L^{-1}$ | 99.3% (140 min) | 203 |
| Sulfadiazine | BC_$TiO_2$_MagEx | Visible light | 5.0 mg $L^{-1}$ | 1.0 g $L^{-1}$ | 76.0% (240 min) | 204 |
| Sulfadiazine | ZIF-67/Ag NPs/$NaYF_4$ : Yb,Er | Simulated sunlight | 10 mg $L^{-1}$ | | 95.4% (180 min) | 205 |

Among these, sulfanilamide, sulfadiazine, sulfamethazine/sulfadimidine, and sulfamethoxazole are frequently used. These contaminants alter the biological population, which could have an adverse effect on human health. Numerous studies indicate that the paths and capabilities of sulfonamide degradation are connected to their substituents.[143] Fig. 5 concludes the sulfonamide degradation routes in different photocatalytic systems. Sulfonamides would degrade primarily due to sulfonamide cleavage of the S–N and C–N bonds, amino group oxidation, hydroxylation, and cleavage of the S–C bond between the sulphur and benzene ring by attacking radicals, which would progressively produce the corresponding byproducts.[77] Table 3 provides an overview of the results of the efficient degradation of sulphonamides using semiconductor photocatalytic technology.

### 5.3. Photocatalytic degradation of fluoroquinolones

Since the late 1980s, fluoroquinolones have been used as medications for humans and animals to prevent bacterial infections.[206] Fluoroquinolones are found in the environment in significant amounts due to animal waste from farms, human waste from residential areas and hospitals, and fertiliser dispersal in agriculture. Generally, fluoroquinolones are prepared primarily by adding fluorine and piperazine groups to form the quinolones core structure[207] in which ciprofloxacin, norfloxacin, levofloxacin/ofloxacin, enrofloxacin are the common used fluoroquinolones.[208,209] Since their longer half-life (10.6 days in surface water and 580 days in sediments), more than 70% fluoroquinolones are discharged unmetabolized.[210] Moreover, due to their chemical stability, these fluoroquinolones are hard to be degraded thoroughly in the environment, which have potential harm to the ecological environment.[209]

Recent studies have demonstrated the development of highly effective photocatalytic devices for fluoroquinolone degradation. Table 4 displays the outcomes. The fluoroquinolone contaminants are discovered to be efficiently destroyed in the presence of light by employing photocatalysts. The chemical structures of fluoroquinolones and the conditions under which photocatalytic processes occur can be responsible for significant modification in the degradation capacity of fluoroquinolones by various photocatalytic processes.[77] Fig. 6, comprises the fluoroquinolone degradation pathways under various photocatalytic processes.

### 5.4. Photocatalytic degradation of macrolides

Macrolides are monocyclic lactones with a high substitution rate having potency to prevent the synthesis of proteins.[291] They belong to the class of large-ringed natural lactones, which typically have 12, 14, or 16 members. Examples of these lactones are tylosin, erythromycin, spiramycin, oleandomycin, clarithromycin, and azithromycin.[292] Macrolides are not completely eradicated in sewage treatment plants, and it has been revealed that they do not readily hydrolyze in the environment,

 

Table 4 Photocatalytic degradation of fluoroquinolones at different conditions

| | | | Optimum conditions | | | |
|---|---|---|---|---|---|---|
| Target antibiotic | Photocatalyst | Source of light | Initial concentration | Catalyst concentration | Degradation (%) | Ref. |
| Ciprofloxacin | $Ag/SiO_2$ | Sunlight | 10.0 mg $L^{-1}$ | 0.12 g $L^{-1}$ | 98.0% (180 min) | 211 |
| Ciprofloxacin | ZnO/CD | Sunlight | 10.0 mg $L^{-1}$ | 0.6 g $L^{-1}$ | 98.0% (110 min) | 212 |
| Ciprofloxacin | $NCuTiO_2$/CQD | Visible light | 20.0 mg $L^{-1}$ | 0.8 g $L^{-1}$ | 89.0% (180 min) | 213 |
| Ciprofloxacin | $ZnO/Co_3O_4$ | Visible light | 10.0 mg $L^{-1}$ | 2.4 g $L^{-1}$ | 100% (30 min) | 214 |
| Ciprofloxacin | $TiO_2$/Ce | UV light | 40.0 mg $L^{-1}$ | 6.0 g $L^{-1}$ | 93.0% (180 min) | 215 |
| Ciprofloxacin | $TiO_2/WO_3$ | UV light | 20.0 mg $L^{-1}$ | 0.5 g $L^{-1}$ | 100% (120 min) | 216 |
| Ciprofloxacin | CuO | Visible light | 10.0 mg $L^{-1}$ | 5.0 g $L^{-1}$ | 60.0% (300 min) | 217 |
| Ciprofloxacin | $CeO_2/Co_3O_4$ | Visible light | 5.0 mg $L^{-1}$ | 0.5 g $L^{-1}$ | 87.8% (50 min) | 218 |
| Ciprofloxacin | $TiO_2$/N | UV light | 30.0 mg $L^{-1}$ | 1.0 g $L^{-1}$ | 94.5% (120 min) | 219 |
| Ciprofloxacin | $TiO_2$/La (0.1%) | Visible light | 10.0 mg $L^{-1}$ | 0.6 g $L^{-1}$ | 99.5% (300 min) | 220 |
| Ciprofloxacin | $TiO_2$/Sm (0.1%) | Visible light | 10.0 mg $L^{-1}$ | 0.9 g $L^{-1}$ | 99.0% (300 min) | 221 |
| Ciprofloxacin | $TiO_2$/Er (0.1%) | Visible light | 10.0 mg $L^{-1}$ | 0.9 g $L^{-1}$ | 99.0% (300 min) | 221 |
| Ciprofloxacin | ZnO/Nd (0.1%) | Visible light | 6.0 mg $L^{-1}$ | 0.9 g $L^{-1}$ | 99.0% (120 min) | 222 |
| Ciprofloxacin | $Fe_3O_4/Bi_2WO_6$ | Visible light | 10.0 mg $L^{-1}$ | 0.3 g $L^{-1}$ | 99.7% (25 min) | 223 |
| Ciprofloxacin | $MMT/CuFe_2O_4$ | UV light | 32.5 mg $L^{-1}$ | 0.78 g $L^{-1}$ | 80.0% (47.5 min) | 224 |
| Ciprofloxacin | Au-RGO/$TiO_2$ | Visible light | 10.0 mg $L^{-1}$ | | 96.93% (180 min) | 225 |
| Ciprofloxacin | $CeO_2$/ZnO | UV light | 10.0 mg $L^{-1}$ | 0.25 g $L^{-1}$ | 92.0% (360 min) | 226 |
| Ciprofloxacin | $MgFe_2O_4$/UiO-67 | Visible light | 10.8 mg $L^{-1}$ | | 99.62% (90 min) | 227 |
| Ciprofloxacin | $B_2O_3$/N-rGO | Visible light | 15.0 mg $L^{-1}$ | 0.25 g $L^{-1}$ | 98.0% (180 min) | 228 |
| Ciprofloxacin | $rGO/Bi_4O_5Br_2$ | Visible light | 10.0 mg $L^{-1}$ | 0.5 g $L^{-1}$ | 97.6% (60 min) | 229 |
| Ciprofloxacin | CdS@CuS/rGO | Visible light | 10.0 mg $L^{-1}$ | 0.25 g $L^{-1}$ | 91.5% (60 min) | 230 |
| Ciprofloxacin | NiAl LDH/$Fe_3O_4$–rGO | Visible light | 10.0 mg $L^{-1}$ | 0.25 g $L^{-1}$ | 91.36% (150 min) | 231 |
| Ciprofloxacin | $Ag_2MoO_4$ | UV light | 20.0 mg $L^{-1}$ | 0.5 g $L^{-1}$ | 98.0% (40 min) | 232 |
| Ciprofloxacin | SiC/g-$C_3N_4$ | Visible light | 10.0 mg $L^{-1}$ | 0.4 g $L^{-1}$ | 95.0% (30 min) | 233 |
| Ciprofloxacin | $B_{0.8}Ce_{0.2}TiO_2$/EPS film | Sunlight | 10.0 mg $L^{-1}$ | 1.0 g $L^{-1}$ | 89.17% (240 min) | 234 |
| Ciprofloxacin | rGO–$ZrO_2$ | Sunlight | 10.0 mg $L^{-1}$ | | 93.1% (240 min) | 235 |
| Ciprofloxacin | $SnO_2$ | UV light | 50.0 mg $L^{-1}$ | 0.5 g $L^{-1}$ | 99.7% (120 min) | 236 |
| Ciprofloxacin | BFO/biochar | Solar light | 10.0 mg $L^{-1}$ | 2.0 g $L^{-1}$ | 70.4% (120 min) | 237 |
| Ciprofloxacin | g-$C_3N_4/Fe_2O_3$ | UV light | 10.0 mg $L^{-1}$ | 0.3 g $L^{-1}$ | 100% (60 min) | 238 |
| Ciprofloxacin | $Bi_2O_2CO_3$ | Visible light | 10.0 mg $L^{-1}$ | 1.0 g $L^{-1}$ | 76.8% (60 min) | 239 |
| Ciprofloxacin | $Bi_2WO_6/BiO_{2-x}$ | Visible light | 10.0 mg $L^{-1}$ | 0.5 g $L^{-1}$ | 91.8% (120 min) | 240 |
| Ciprofloxacin | GO@$Fe_3O_4$@$TiO_2$ | Visible light | 10.0 mg $L^{-1}$ | 0.1 g $L^{-1}$ | 91.5% (240 min) | 241 |
| Ciprofloxacin | MIL-68(In, Bi)–$NH_2$@BiOBr | Visible light | 5.0 mg $L^{-1}$ | 0.35 g $L^{-1}$ | 91.1% (90 min) | 242 |
| Ciprofloxacin | $Sm_2O_3/In_2S_3$ | Visible light | 20.0 mg $L^{-1}$ | 0.05 g $L^{-1}$ | 99.4% (55 min) | 243 |
| Ciprofloxacin | ZnCrLDO/FA | Visible light | 10.0 mg $L^{-1}$ | | 98.0% (120 min) | 244 |
| Ciprofloxacin | 2D $Bi_2O_2CO_3$ | UV-vis light | 10.0 mg $L^{-1}$ | 1.0 g $L^{-1}$ | 76.8% (60 min) | 245 |
| Ciprofloxacin | $In_2O_3$/BiOBr | Visible light | 10.0 mg $L^{-1}$ | | 93.5% (90 min) | 246 |
| Ciprofloxacin | BiOI/MOF/F-BC | Simulated sunlight | 10.0 mg $L^{-1}$ | | 94.4% (180 min) | 247 |
| Ciprofloxacin | BiOCl/diatomite | Simulated sunlight | 10.0 mg $L^{-1}$ | 0.5 g $L^{-1}$ | 94.0% (10 min) | 248 |
| Ciprofloxacin | $Ti_3C_2$–Bi/BiOCl | Visible light | 20.0 mg $L^{-1}$ | 1.0 g $L^{-1}$ | 89.0% (100 min) | 249 |
| Ciprofloxacin | 3D tripyramid $TiO_2$ | Simulated sunlight | 10.0 mg $L^{-1}$ | 1.0 g $L^{-1}$ | 90.0% (60 min) | 250 |
| Ciprofloxacin | $ZnSnO_3$ | Simulated sunlight | 10.0 mg $L^{-1}$ | 0.5 g $L^{-1}$ | 85.9% (100 min) | 251 |
| Ciprofloxacin | ZnO–$SnO_2$–$Zn_2SnO_4$ | Simulated sunlight | 10.0 mg $L^{-1}$ | 0.5 g $L^{-1}$ | 95.8% (80 min) | 252 |
| Levofloxacin | $WO_{12}$/g-$C_3N_4$ | Visible light | 10.0 mg $L^{-1}$ | | 90.8% (70 min) | 253 |
| Levofloxacin | Au@ZnONPs-$MoS_2$-rGO | Visible light | 10.0 mg $L^{-1}$ | 1.0 g $L^{-1}$ | 99.8% (120 min) | 254 |
| Levofloxacin | $LaFeO_3$/CdS | Visible light | 10.0 mg $L^{-1}$ | | 97.3% (100 min) | 255 |
| Levofloxacin | Fe-doped BiOCl | Visible light | 15.0 mg $L^{-1}$ | 0.5 g $L^{-1}$ | 94.7% (60 min) | 256 |
| Levofloxacin | Mn-doped $ZnIn_2S_4$ | Visible light | 10.0 mg $L^{-1}$ | | 100% (30 min) | 257 |
| Levofloxacin | g-$C_3N_4/TiO_2$ | Solar light and UV irradiation | 5.0 mg $L^{-1}$ | 0.5 g $L^{-1}$ | 100% (50 min) | 258 |
| Levofloxacin | $WO_3/TiO_2$ | Solar and UV light | 5.0 mg $L^{-1}$ | 0.5 g $L^{-1}$ | 66.0% (50 min) | 258 |
| Levofloxacin | $Sb_2S_3/In_2S_3/TiO_2$ | Visible light | 10.0 mg $L^{-1}$ | | 86.7% (160 min) | 259 |
| Levofloxacin | Fe–ZnO/$WO_3$ | Visible light | 10.0 mg $L^{-1}$ | 0.5 g $L^{-1}$ | 96.0% (60 min) | 260 |
| Levofloxacin | $Co_3O_4/Bi_2MoO_6$@ g-$C_3N_4$ | Visible light | 10.0 mg $L^{-1}$ | | 95.21% | 261 |
| Levofloxacin | $Bi_2O_2CO_3/Ti_3C_2T_x$ | Visible light | 10.0 mg $L^{-1}$ | | 95.4% (80 min) | 262 |
| Ofloxacin | g-$C_3N_4$/$NH_2$-MIL-88B(Fe) | Visible light | 10.0 mg $L^{-1}$ | 0.4 g $L^{-1}$ | 96.5% (150 min) | 263 |
| Ofloxacin | TS-1/$C_3N_4$ | Visible light | 10.0 mg $L^{-1}$ | 1.55 g $L^{-1}$ | 90.0% (70 min) | 264 |
| Ofloxacin | $BiFeO_3$ | Visible light | 10.0 mg $L^{-1}$ | 0.5 g $L^{-1}$ | 80.0% (180 min) | 265 |
| Ofloxacin | Mg–Ni co-doped $TiO_2$ | Visible light | 40.0 mg $L^{-1}$ | 2.0 g $L^{-1}$ | 96.0% (60 min) | 266 |
| Ofloxacin | PEB-DBT/α-$Fe_2O_3$ | Visible light | 40.0 mg $L^{-1}$ | | 98.0% (50 min) | 267 |
| Ofloxacin | UiO-66/wood | Simulated sunlight | 10.0 mg $L^{-1}$ | 0.02 g $L^{-1}$ | 80.96% (270 min) | 268 |
| Ofloxacin | $ZnFe_2O_4/BiVO_4$ | Visible light | 20.0 mg $L^{-1}$ | 1.0 g $L^{-1}$ | 97.0% (30 min) | 269 |

Table 4 (*Contd.*)

| Target antibiotic | Photocatalyst | Source of light | Optimum conditions | | Degradation (%) | Ref. |
|---|---|---|---|---|---|---|
| | | | Initial concentration | Catalyst concentration | | |
| Ofloxacin | $Ag_2O$-g-$C_3N_4$ | Visible light | 10.0 mg $L^{-1}$ | 0.5 g $L^{-1}$ | 99.1% (15 min) | 270 |
| Norfloxacin | AgI/BiOI | Visible light | 20.0 mg $L^{-1}$ | 1.0 g $L^{-1}$ | 98.8% (120 min) | 271 |
| Norfloxacin | $Fe_3O_4$@La–$BiFeO_3$ | Visible light | 10.0 mg $L^{-1}$ | | 93.8% (60 min) | 272 |
| Norfloxacin | Y–$TiO_2$/5A/$NiFe_2O_4$ | Visible light | 30.0 mg $L^{-1}$ | 2.0 g $L^{-1}$ | 96.55% (60 min) | 273 |
| Norfloxacin | AgI/BiOI | Visible light | 10.0 mg $L^{-1}$ | 1.0 g $L^{-1}$ | 98.8% (120 min) | 274 |
| Norfloxacin | $Ni_2O_3$@PC | UV light | 10.0 mg $L^{-1}$ | 0.1 g $L^{-1}$ | 59.0% (180 min) | 275 |
| Norfloxacin | ZnO/g-$C_3N_4$ | Visible light | 15.0 mg $L^{-1}$ | 1.8 g $L^{-1}$ | 92.8% (120 min) | 276 |
| Norfloxacin | RGO–SnSe | Visible light | 40.0 mg $L^{-1}$ | 1.0 g $L^{-1}$ | 90.7% (70 min) | 277 |
| Norfloxacin | $SnS_2$ | Solar light | 20.0 mg $L^{-1}$ | 0.05 g $L^{-1}$ | 80.0% (110 min) | 278 |
| Norfloxacin | $Cu_2O$@$WO_3$ | Visible light | 10.0 mg $L^{-1}$ | 0.2 g $L^{-1}$ | 90.0% (90 min) | 279 |
| Norfloxacin | Fe(III)–$SrTiO_3$-GO | Visible light | 10.0 mg $L^{-1}$ | | 92.3% (120 min) | 280 |
| Norfloxacin | GCNQDs/$Ni_5P_4$ | UV light | 40.0 mg $L^{-1}$ | 0.1 g $L^{-1}$ | 92.0% (120 min) | 281 |
| Norfloxacin | BiOCl/ZnS–$V_{Zn+O}$ | Visible light | 20.0 mg $L^{-1}$ | 0.5 g $L^{-1}$ | 97.9% (50 min) | 282*a* |
| Norfloxacin | Au/MIL-101(Fe)/BiOBr | Visible light | 10.0 mg $L^{-1}$ | 0.1 g $L^{-1}$ | 100% (20 min) | 282*b* |
| Enrofloxacin | Strontium-doped $TiO_2$/CDs | Visible light | 10.0 mg $L^{-1}$ | 0.05 g $L^{-1}$ | 84.7% (70 min) | 283 |
| Enrofloxacin | Ag–$ZnFe_2O_4$–rGO | Visible light | 10.0 mg $L^{-1}$ | | 99.1% (60 min) | 284 |
| Enrofloxacin | $C_{sx}WO_3$/BiOI | Visible light | 10.0 mg $L^{-1}$ | 0.5 g $L^{-1}$ | 100% (60 min) | 285 |
| Enrofloxacin | Zero-valent copper (nZVC) | Visible light | 10.0 mg $L^{-1}$ | 0.5 g $L^{-1}$ | 99.51% (70 min) | 286 |
| Enrofloxacin | CdS/CuAg | Visible light | 10.0 mg $L^{-1}$ | 0.02 g $L^{-1}$ | 99.9% (45 min) | 287 |
| Enrofloxacin | $Fe_{3-x}S_{4-y}$/g-$C_3N_4$ | Visible light | 10.0 mg $L^{-1}$ | 0.5 g $L^{-1}$ | 100% (30 min) | 288 |
| Enrofloxacin | P/O co-doped g-$C_3N_4$/$TiO_2$ | Visible light | 10.0 mg $L^{-1}$ | 1.0 g $L^{-1}$ | 98.5% (60 min) | 289 |
| Enrofloxacin | Ball-milled biochar | Visible light | 20.0 mg $L^{-1}$ | 0.2 g $L^{-1}$ | 80.2% (150 min) | 290*a* |
| Enrofloxacin | MIL-101(Fe)/BiOBr | Visible light | 10.0 mg $L^{-1}$ | 0.1 g $L^{-1}$ | 84.4% (40 min) | 290*b* |

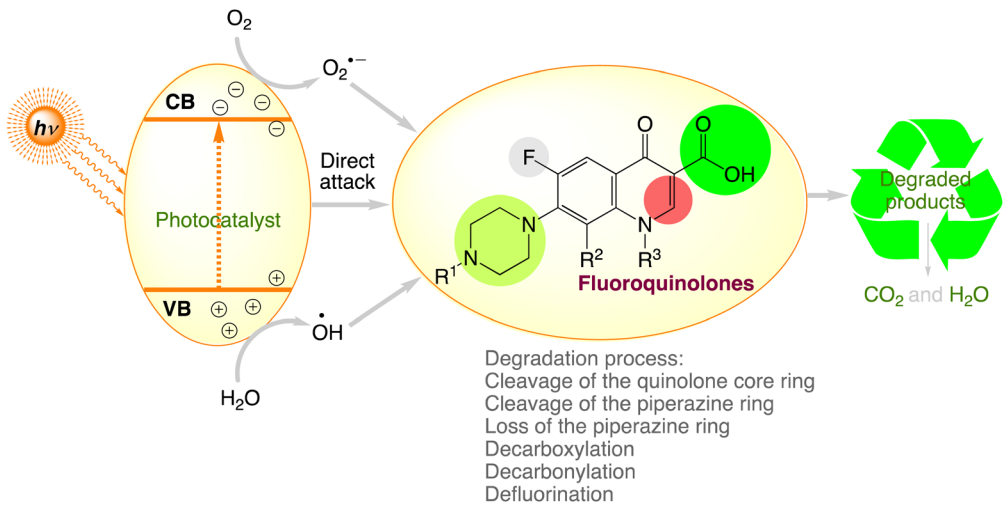


Fig. 6 The proposed photocatalytic degradation pathways of fluoroquinolones.

suggesting that they may continue to exist in the environment. Thus, it is important that we pay attention to the issue of macrolides causing environmental contamination.[293] Tylosin is the most often utilised agent among macrolides, and one of the best technologies for their removal is photocatalytic oxidation.[77,294] The photodegradation of macrolides by various photocatalysts can be briefly summarized in the Fig. 7. When a photon flows surpassing a semiconductor's band gap, an electron ($e^-$) moves from the valence band (VB) to the conduction band (CB), generating a photogenerated hole on the VB. The chemical reaction will then occur when the separated charge carriers diffuse into the semiconductor/liquid interface's catalytically active regions (Fig. 7).

Three types of radicals can be formed by holes: (1) directly oxidising macrolides into certain byproducts; (2) reacting with $H_2O$ to generate hydroxyl radicals ($^{\cdot}OH$) with high oxidation potential; and (3) reacting with $O_2$ to form superoxide radicals ($O_2^{-\cdot}$) with significant reducibility of electrons. In the end, these produced oxidation radicals can break down macrolides into hazardous or harmless byproducts, which can then be broken down further into $CO_2$ and $H_2O$ by extending the reaction period. According to numerous research conducted recently,

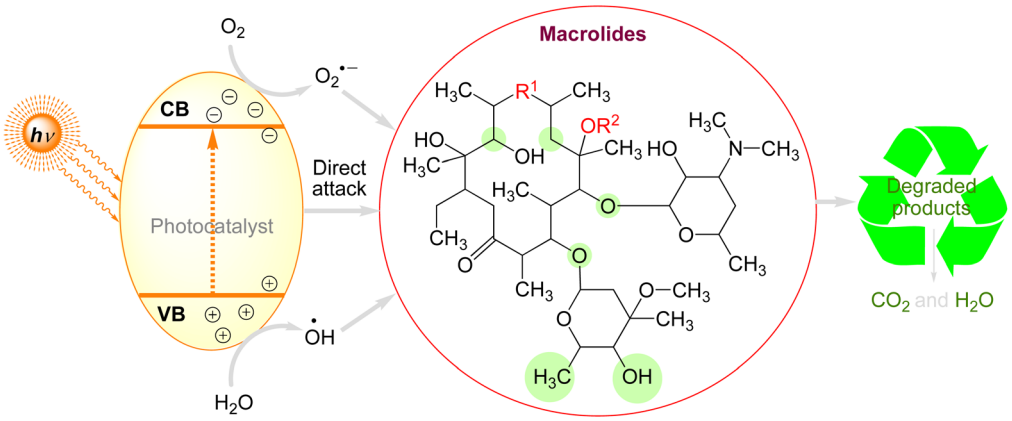


Fig. 7 The proposed photocatalytic degradation pathways of macrolides.

photocatalytic oxidation technologies are an excellent way to treat macrolides. Unfortunately, not much research has been done to fully understand how macrolides' complicated structure and enormous molecular weight affect their degradation processes. Table 5 summarises the photocatalytic degradation of macrolides under various circumstances.

### 5.5. Photocatalytic degradation of β-lactams

β-Lactams as broad-spectrum antibiotics that are mainly classified as penicillin and cephalosporin. Amoxicillin (AMX) and ampicillin (AMP) are examples of penicillins that are generated from penicillium and have the ability to prevent amino acid chains in bacterial cell walls from cross-linking. The semi-synthetic antibiotic class referred to as cephalosporins, which includes ceftiofur sodium (CFS), ceftriaxone sodium, cephalexin (CLX), and other similar antibiotics, is derived from 7-aminocephalosporanic acid (7-ACA).[77,317,318]

Investigations have shown that municipal wastewater treatment plants[319] have greater quantities of penicillin and cephalosporin. β-Lactams, on the other hand, were not expected to survive in the environment because of their strong polarity, reduced adsorption capacity, and capacity to hydrolyze to the soil. Fig. 8 summarises the processes *via* which various, β-lactam antibiotics degrade. Table 6 summarises the results of the photocatalytic degradation of β-lactams using various photocatalysts.

Table 5 Photocatalytic degradation of macrolides at different conditions

| | | | Optimum conditions | | | |
|---|---|---|---|---|---|---|
| Target antibiotic | Photocatalyst | Source of light | Initial concentration | Catalyst concentration | Degradation (%) | Ref. |
| Tylosin | ZnCrNi/GO | Visible light | 10.0 mg $L^{-1}$ | | 90.0% (80 min) | 295 |
| Tylosin | Au/$TiO_2$-CCBs | Visible light | | | 92.0% (180 min) | 296 |
| Tylosin | $TiO_2$ | UV light | 20 mg $L^{-1}$ | 0.1 g $L^{-1}$ | 80.0% (300 min) | 297 |
| Tylosin | g-$C_3N_4$ | Simulated sunlight | 5 mg $L^{-1}$ | 0.05 g $L^{-1}$ | 99.0% (30 min) | 298 |
| Tylosin | Sm-doped g$C_3N_4$ | Simulated sunlight | 25 mg $L^{-1}$ | 0.5 g $L^{-1}$ | 78.4% (90 min) | 299 |
| Tylosin | Er-doped g-$C_3N_4$ | Simulated sunlight | 25 mg $L^{-1}$ | 0.5 g $L^{-1}$ | 70% (90 min) | 300 |
| Tylosin | Goethite-modified $C_3N_4$/$ZnFe_2O_4$ | Simulated sunlight | 5 mg $L^{-1}$ | 0.5 g $L^{-1}$ | 99.0% (30 min) | 301 |
| Erythromycin | $SnO_2$-doped $TiO_2$ | Visible light | 50 mg $L^{-1}$ | 0.5 g $L^{-1}$ | 67.0% (240 min) | 302 |
| Erythromycin | $CaCO_3$ (nano-calcite) | Sunlight | 30 mg $L^{-1}$ | 0.5 g $L^{-1}$ | 93.0% (360 min) | 303 |
| Erythromycin | Graphene-based $TiO_2$ | Simulated sunlight | 0.10 mg $L^{-1}$ | 0.1 g $L^{-1}$ | 84.0% (60 min) | 304 |
| Erythromycin | $TiO_2$ | UV light | 10 mg $L^{-1}$ | 0.25 g $L^{-1}$ | 90.0% (250 min) | 305 |
| Erythromycin | g-$C_3N_4$/CdS | Simulated sunlight | 50 mg $L^{-1}$ | 0.5 g $L^{-1}$ | 81.02% (60 min) | 306 |
| Erythromycin | $ZnIn_2S_4$ | Visible light | 10 mg $L^{-1}$ | 0.05 g $L^{-1}$ | 100% (180 min) | 307 |
| Spiramycin | $TiO_2$ | UV light | 25 mg $L^{-1}$ | 0.25 g $L^{-1}$ | 100% (180 min) | 308 |
| Spiramycin | $TiO_2$ and ZnO | UV/Visible light | 10 mg $L^{-1}$ | 0.05 g $L^{-1}$ | 100% (120 min) | 309 |
| Spiramycin | N-doped $TiO_2$ | Visible light | 40 mg $L^{-1}$ | 3.0 g $L^{-1}$ | 74.0% (240 min) | 310 |
| Spiramycin | g-$C_3N_4$/$ZnFe_2O_4$ | Visible light | 20 mg $L^{-1}$ | 1.0 g $L^{-1}$ | 95.0% (240 min) | 311 |
| Clarithromycin | Graphene-based $TiO_2$ | Simulated sunlight | 0.10 mg $L^{-1}$ | 0.1 g $L^{-1}$ | 86.0 (60 min) | 312 |
| Azithromycin | $ZrO_2$/Ag/$TiO_2$ | Visible light | 20 mg $L^{-1}$ | 0.2 g $L^{-1}$ | 90% (9 h) | 313 |
| Azithromycin | GO/$Fe_3O_4$/ZnO/$SnO_2$ | UV light | 30 mg $L^{-1}$ | 1.0 g $L^{-1}$ | 90.06% (120 min) | 314 |
| Azithromycin | Doped $TiO_2$/fberglass-rubberized silicone | UV light | 250 mg $L^{-1}$ | 0.02 g $L^{-1}$ | 70.0% (15 min) | 315 |
| Azithromycin | PAC/Fe/Ag/Zn | UV light | 40 mg $L^{-1}$ | 0.04 g $L^{-1}$ | 99.5% (120 min) | 316 |

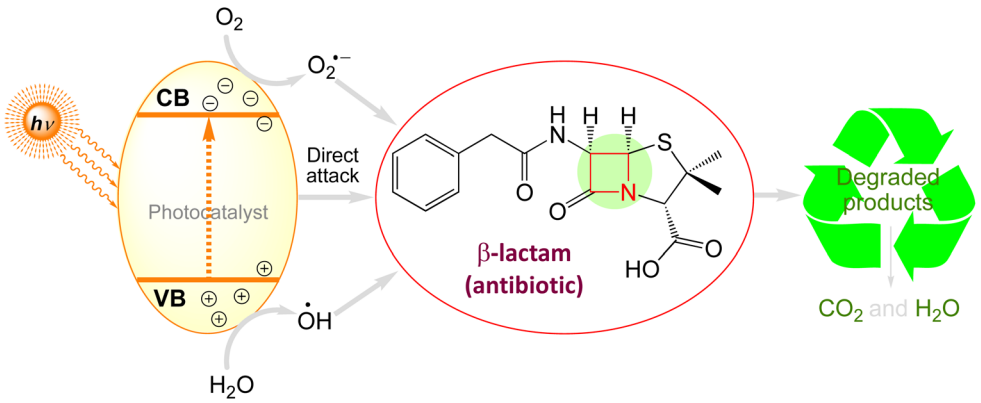


Fig. 8 The proposed photocatalytic degradation pathways of β-lactams (antibiotics).

Table 6 Photocatalytic degradation of β-lactams (antibiotics) at different conditions

| | | | Optimum conditions | | | |
|---|---|---|---|---|---|---|
| Target antibiotic | Photocatalyst | Source of light | Initial concentration | Catalyst concentration | Degradation (%) | Ref. |
| Amoxicillin | $Fe_3O_4$@void@CuO/ZnO | Visible light | 10.0 mg $L^{-1}$ | | 100% (70 min) | 320 |
| Amoxicillin | Iron nanoparticle (IPP) | Visible light | 10.0 mg $L^{-1}$ | 2.5 g $L^{-1}$ | 60.0% (60 min) | 321 |
| Amoxicillin | $TiO_2$–Cr | Visible light | 10 mg $L^{-1}$ | 0.33 g $L^{-1}$ | 100% (90 min) | 322 |
| Amoxicillin | CuI/$FePO_4$ | Visible light | 10 mg $L^{-1}$ | | 90.0% (60 min) | 323 |
| Amoxicillin | GO/$TiO_2$ | UV light | 50 mg $L^{-1}$ | 0.6 g $L^{-1}$ | 99.84% (60 min) | 324 |
| Amoxicillin | CN-T | Visible light | 50 mg $L^{-1}$ | 0.3 g $L^{-1}$ | 100% (48 h) | 325 |
| Amoxicillin | Magnetite/SCB biochar | Visible light | 100 mg $L^{-1}$ | 0.12 g $L^{-1}$ | 73.51% (240 min) | 326 |
| Amoxicillin | $TiO_2$@nZVI/PS | Visible light | 20 mg $L^{-1}$ | 1.0 g $L^{-1}$ | 99.0% (60 min) | 327 |
| Amoxicillin | Ni doped ZnO | UV-visible light | 10 mg $L^{-1}$ | | 86.21% (120 min) | 328 |
| Amoxicillin | ZnONPs | UV light | 100 mg $L^{-1}$ | 0.2 g $L^{-1}$ | 90.0% (120 min) | 329 |
| Amoxicillin | $TiO_2$/$Fe_2O_3$ | Solar light | 50 mg $L^{-1}$ | 1.0 g $L^{-1}$ | 100% (180 min) | 330 |
| Amoxicillin | MIL-53(Al)/ZnO | Visible light | 10 mg $L^{-1}$ | 1.0 g $L^{-1}$ | 100% (60 min) | 331 |
| Amoxicillin | Mn-doped $Cu_2O$ | Sunlight | 15 mg $L^{-1}$ | 1.0 g $L^{-1}$ | 92.0% (180 min) | 332 |
| Amoxicillin | $WO_3$ | Simulated sunlight | 20 mg $L^{-1}$ | 0.104 g $L^{-1}$ | 99.99% (180 min) | 333 |
| Amoxicillin | $TiO_2$ | UV light | 10 mg $L^{-1}$ | 0.25 g $L^{-1}$ | 65.0% (150 min) | 334 |
| Amoxicillin | ZnO@$TiO_2$ | Visible light | 10 mg $L^{-1}$ | 0.1 g $L^{-1}$ | 80.0% (70 min) | 335 |
| Amoxicillin | Mesoporous g-$C_3N_4$ | Visible light | 2 mg $L^{-1}$ | 1.0 g $L^{-1}$ | 99% (60 min) | 336 |
| Amoxicillin | Ag/$TiO_2$/Mesoporous g-$C_3N_4$ | Visible light | 5 mg $L^{-1}$ | 1.0 g $L^{-1}$ | 99% (60 min) | 337 |
| Amoxicillin | $BiVO_4$ | Visible light | 5 mg $L^{-1}$ | | 97.45% (90 min) | 338 |
| Amoxicillin | C-dots/$Sn_2Ta_2O_7$/$SnO_2$ | Simulated sunlight | 20 mg $L^{-1}$ | | 88.3% (120 min) | 339 |
| Ceftiofur sodium | $CdFe_2O_4$/g-$C_3N_4$ | Visible light | 30 mg $L^{-1}$ | | 68.6% (60 min) | 340 |
| Ceftiofur sodium | Ag–ZnO | Visible light | 10 mg $L^{-1}$ | | 89.0% (6 h) | 341 |
| Ceftiofur sodium | Ag–$TiO_2$ | Visible light | 10 mg $L^{-1}$ | | 92.0% (90 min) | 342 |
| Ceftriaxone sodium | g-$C_3N_4$–ZnO | UV light | 10 mg $L^{-1}$ | | 100% (60 min) | 343 |
| Ceftriaxone sodium | ZnO/$ZnIn_2S_4$ | Visible light | 10 mg $L^{-1}$ | 0.4 g $L^{-1}$ | 83.5% (150 min) | 344 |
| Ceftriaxone sodium | CdS-g-$C_3N_4$ | Visible light | 15 mg $L^{-1}$ | 0.06 g $L^{-1}$ | 92.55% (81 min) | 345 |
| Ceftriaxone sodium | CdSe QDs@$MoS_2$ | UV light | 20 mg $L^{-1}$ | 0.012 g $L^{-1}$ | 85.47% (180 min) | 346 |
| Cephalexin | ZnO | Simulated sunlight | 20 mg $L^{-1}$ | 0.1 g $L^{-1}$ | 96.0% (25 min) | 347 |
| Cephalexin | Sodium persulfate (SPS) and fenton | UV light | 10 mg $L^{-1}$ | 0.1 g $L^{-1}$ | 100% (60 min) | 348 |
| Cephalexin | g-$C_3N_4$/Zn doped $Fe_3O_4$ | Visible light | 10 mg $L^{-1}$ | | 91.0% (5 h) | 349 |
| Cephalexin | $CeO_2$@$WO_3$ | Visible light | 20 mg $L^{-1}$ | 0.019 g $L^{-1}$ | 98.8% (95 min) | 350 |

### 5.6. Photocatalytic degradation of nitroimidazoles

Nitroimidazoles are widely utilised in both human and veterinary medicine, mostly for the treatment of infectious illnesses. Nitroimidazoles are easily accumulated in hospitals, fish and poultry farms, animal husbandry, and the meat industry due to their high solubility, limited degradability, and carcinogenicity, all of which pose a major concern to human health and the ecosystem. As a result, creating effective strategies for the removal of nitroimidazoles[77,351–354] is crucial. One popular

Table 7 Photocatalytic degradation of nitroimidazoles at different conditions

| Target antibiotic | Photocatalyst | Source of light | Optimum conditions: Initial concentration | Optimum conditions: Catalyst concentration | Degradation (%) | Ref. |
|---|---|---|---|---|---|---|
| Metronidazole | Ag-doped- $Ni_{0.5}Zn_{0.5}Fe_2O_4$ (Ag-d-NZF) | UV light | 50.0 mg $L^{-1}$ | 0.01 g $L^{-1}$ | 99.9% (360 min) | 355 |
| Metronidazole | Ag–N–$SnO_2$ | Visible light | 10.0 mg $L^{-1}$ | 0.4 g $L^{-1}$ | 97.03% (120 min) | 356 |
| Metronidazole | $TiO_2$ decorated magnetic reduced graphene oxide | Visible light | 20.0 mg $L^{-1}$ | 0.75 g $L^{-1}$ | 100% (120 min) | |
| Metronidazole | Co–$TiO_2$/sulphite | Visible light | 20.0 mg $L^{-1}$ | 0.8 g $L^{-1}$ | 94.0% (18 min) | 357 |
| Metronidazole | ZEO/HDTMA-Br/CuS | Simulated sunlight | 10.0 mg $L^{-1}$ | 0.01 g $L^{-1}$ | 100% (180 min) | 358 |
| Metronidazole | Co/g-$C_3N_4$/$Fe_3O_4$ | Visible light | 5.0 mg $L^{-1}$ | 0.7 g $L^{-1}$ | 100% (60 min) | 359 |
| Metronidazole | UiO-66-$NH_2$ | Solar light | 5.0 mg $L^{-1}$ | 0.125 g $L^{-1}$ | 68.0% (360 min) | 360 |
| Metronidazole | PAC/$Fe_3O_4$ | UV light | 30.0 mg $L^{-1}$ | 0.6 g $L^{-1}$ | 99.87% (90 min) | 361 |
| Metronidazole | $ZnFe_2O_4$@Uio-66 | UV light | 90.0 mg $L^{-1}$ | 0.05 g $L^{-1}$ | 93.7% (120 min) | 362 |
| Metronidazole | ZnO/biochar | Visible light | 10.0 mg $L^{-1}$ | | 97.1% (40 min) | 363 |
| Metronidazole | CN–PPy–MMt | Visible light | 10.0 mg $L^{-1}$ | 0.8 g $L^{-1}$ | 99.3% (40 min) | 364 |
| Metronidazole | $TiO_2$–$Fe_3O_4$ | Visible light | 20.0 mg $L^{-1}$ | 1.0 g $L^{-1}$ | 96.0% (180 min) | 365 |
| Metronidazole | SBA-15/$TiO_2$ | UV light | 10.0 mg $L^{-1}$ | 0.5 g $L^{-1}$ | 87.7% (200 min) | 366 |
| Metronidazole | ZnO–$ZnAl_2O_4$ | Sunlight | 20.0 mg $L^{-1}$ | 0.4 g $L^{-1}$ | 50.0% (120 min) | 367 |
| Metronidazole | CuS/NiS | Visible light | 150.0 mg $L^{-1}$ | 0.2 g $L^{-1}$ | 23.31% (120 min) | 368 |
| Metronidazole | $MoS_2$/$Bi_2S_3$ | NIR light | 10 mg $L^{-1}$ | | 91.54% (40 min) | 369 |
| Metronidazole | HKUST-1-based $SnO_2$ | UV/Visible light | 40.0 mg $L^{-1}$ | 2.0 g $L^{-1}$ | 98.0% (240 min) | 370 |
| Metronidazole | $Fe_3O_4$@$SiO_2$@$TiO_2$/rGO | UV light | 10.0 mg $L^{-1}$ | 0.1 g $L^{-1}$ | 94.0% (60 min) | 371 |
| Metronidazole | $TiO_2$ | UV light | 80.0 mg $L^{-1}$ | 0.7 g $L^{-1}$ | 100% (600 min) | 372 |
| Metronidazole | $FeNi_3$/chitosan/BiOI | Simulated sunlight | 20.0 mg $L^{-1}$ | 0.04 g $L^{-1}$ | 100% (200 min) | 373 |
| Metronidazole | $Ag_2S$/$BiVO_4$@α-$Al_2O_3$ | Visible light | 30.0 mg $L^{-1}$ | 1.0 g $L^{-1}$ | 90.5% (120 min) | 374 |
| Tinidazole | rGO/BiOCl | UV light | 18.0 mg $L^{-1}$ | 0.001 g $L^{-1}$ | 97.0% (5 min) | 375 |
| Tinidazole | Co/NCHPs | UV/Visible light | 20.0 mg $L^{-1}$ | | 99.99% (6 min) | 376 |
| Tinidazole | Ag/HAp/$In_2S_3$ QDs | Visible light | 20.0 mg $L^{-1}$ | 0.24 g $L^{-1}$ | 96.32% (30 min) | 377 |
| Ornidazole | $TiO_2$ | UV light | 50.0 mg $L^{-1}$ | 1.0 g $L^{-1}$ | 66.15% (180 min) | 378 |
| Ornidazole | $Y^{3+}$-$Bi_5Nb_3O_{15}$ | Visible light | 20.0 mg $L^{-1}$ | 2.0 g $L^{-1}$ | 90.5% (180 min) | 379 |

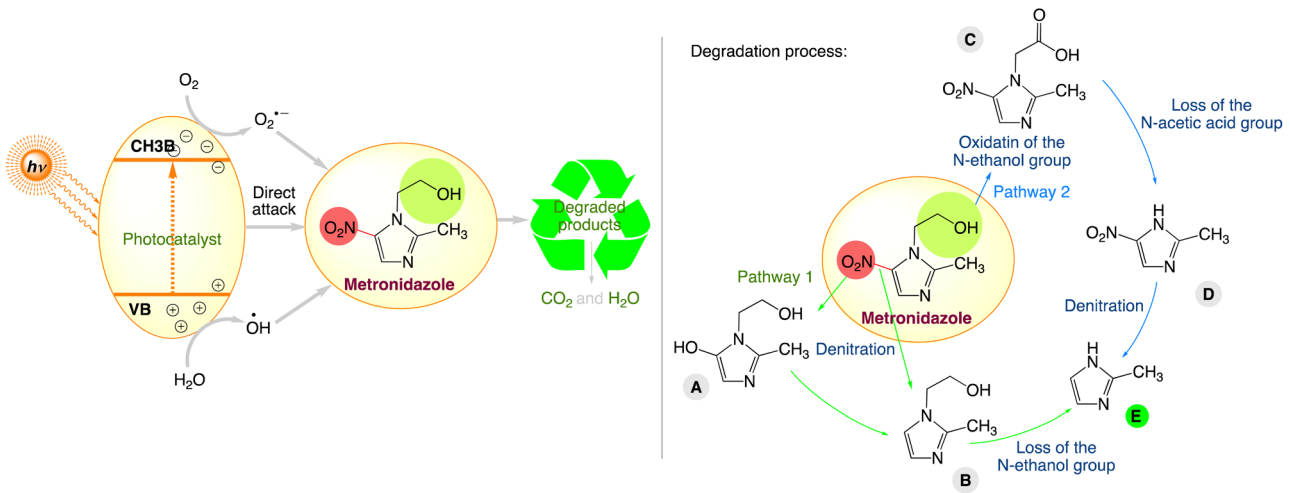


Fig. 9 The proposed photocatalytic degradation pathways of metronidazole.

Table 8 Photocatalytic degradation of other antibiotics at different conditions

| | | | Optimum conditions | | | |
|---|---|---|---|---|---|---|
| Target antibiotic | Photocatalyst | Source of light | Initial concentration | Catalyst concentration | Degradation (%) | Ref. |
| Chloramphenicol | Fe/TaON/β-$Si_3N_4$/β-$Si_3Al_3O_3N_5$ | Visible light | 20.0 mg $L^{-1}$ | 0.01 g $L^{-1}$ | 98.0% (30 min) | 380 |
| Chloramphenicol | $SmVO_4$/g-$C_3N_4$ (SM/CN) | Visible light | 10.0 mg $L^{-1}$ | 0.5 g $L^{-1}$ | 94.35% (105 min) | 381 |
| Chloramphenicol | BiOI/ZnO/rGO | Visible light | 10.0 mg $L^{-1}$ | | 100% (180 min) | 382 |
| Chloramphenicol | $CuInS_2$ | Visible light | 10.0 mg $L^{-1}$ | 0.2 g $L^{-1}$ | 94.3% (120 min) | 383 |
| Chloramphenicol | $Bi_2S_3/ZrO_2$ and $Bi_2WO_6/ZrO_2$ | Visible light | 10.0 mg $L^{-1}$ | 0.2 g $L^{-1}$ | 96.0% (15 min) | 384 |
| Chloramphenicol | PbS/$TiO_2$ | Sunlight | 10.0 mg $L^{-1}$ | 0.06 g $L^{-1}$ | 76.0% (240 min) | 385 |
| Chloramphenicol | rGO–ZnO | UV light | 10.0 mg $L^{-1}$ | 0.5 g $L^{-1}$ | 90.0% (100 min) | 386 |
| Gentamicin | $TiO_2$nps | Visible light | 10.0 mg $L^{-1}$ | | 95.0% (80 min) | 387 |
| Gentamicin | ZnO | UV light | 20.0 mg $L^{-1}$ | 0.2 g $L^{-1}$ | 93.0% (30 min) | 388 |
| Lincomycin | O-g/$C_3N_4$ | Visible light | 100.0 mg $L^{-1}$ | | 99.0% (180 min) | 389 |
| Lincomycin | TNWs/TNAs | Visible light | 500.0 mg $L^{-1}$ | | 85.0% (20 min) | 390 |
| Vancomycin | TNWs/TNAs | Visible light | 500.0 mg $L^{-1}$ | | 100% (20 min) | 390 |
| Vancomycin | $TiO_2$ | UV light | 58.2 mg $L^{-1}$ | 0.23 g $L^{-1}$ | 93.0% (36.3 min) | 391 |
| Vancomycin | $TiO_2$–clinoptilolite | UV light | 30.0 mg $L^{-1}$ | 0.2 g $L^{-1}$ | 97.0% (50.9 min) | 392 |

method for treating nitroimidazoles is photocatalysis. The three most used nitroimidazoles are ornidazole, tinidazole, and metronidazole. The photocatalytic degradation and routes associated with metronidazole have been the subject of the greatest research among them. Table 7 provides an overview of the data from current investigations on the photocatalytic degradation of nitroimidazole.

Further observation from these investigations shows that the nitroimidazole degradation routes are comparable and may be summed up as denitration and the removal of their unique substituents. For instance, Fig. 9 illustrates the various stages of the metronidazole degradation process during the majority of the photocatalytic oxidation process. Three different reaction products were suggested for each of the two metronidazole degradation pathways. In pathway 1, metronidazole undergoes denitration and then loss of *N*-ethanol group, with the generation of products A, B, and E, respectively. In pathway 2, the *N*-ethanol group is first oxidized to carboxyl to produce C, which converts to D through loss of the *N*-acetic acid group. Besides, product D further transforms to E by denitration.

### 5.7. Photocatalytic degradation of other antibiotics

Apart from the previously stated antibiotic, some research continues to concentrate on the photocatalytic breakdown of antibiotics such as lincomycin, glycopeptides, aminoglycosides, and chloramphenicol. Table 8 provides an overview of the data regarding photocatalytic degradation of these antibiotics.

## 6. Conclusions and perspective

The extensive discovery and application of antibiotics in recent decades has impacted human health and environmental systems to some extent. Antibiotic contamination has become a more significant scientific and practical issue overall. Since previous research has already acquired significant fundamental scientific and technical expertise, the photocatalytic technique represents an intriguing promise for attaining the elimination of antimicrobial contaminants. We are able to choose this technology for both indoor and outdoor water treatment systems owing to the freedom in selecting light sources. In addition, it is an industry-friendly technology because it is feasible to use sunlight. Photoscatalysis is a cost-effective method since it requires less space and maintenance than biodegradation. This review therefore provides an overview of the most recent advancements in the photocatalytic degradation of different antibiotics including tetracycline, sulfonamide, fluoroquinolones, macrolides, β-lactams, nitroimidazoles as well as miscellaneous antibiotics in aqueous solution under various reaction circumstances and critically examines recent methods for photocatalytic antibiotic degradation by involving the doping of metal and non-metal into ultraviolet light-driven photocatalysts, the generation of new semiconductor photocatalysts, the development of heterojunction photocatalysts, the building of surface plasmon resonance-enhanced photocatalytic systems that offers a basic understanding of the photocatalytic water treatment process. Utilising solar energy to reduce antimicrobial contaminants through photocatalytic technologies is promising from an industrialization and commercialization standpoint. A useful strategy for increasing photocatalytic activity, decreasing photogenerated carrier recombination, and improving charge separation and transfer efficiency at the photocatalyst interface is the development of heterojunctions. Building several heterojunctions with various semiconductors is therefore a typical tactic. As a result, due to their exceptional photocatalytic activity and acceptable redox ability, heterojunction photocatalysts have gained a lot of interest recently. The development of these photocatalysts on a wide scale and the formation of more efficient photocatalytic water purification systems will be greatly facilitated by future advancements.

## Data availability

No primary research results, software or code have been included and no new data were generated or analysed as part of this review.

## Conflicts of interest

There are no conflicts to declare.

## References

1 J. Niu, K. Wang, Z. Ma, F. Yang and Y. Zhang, *ChemistrySelect*, 2022, **5**, 12353–12364.
2 D. W. Graham, S. Olivares-Rieumont, C. W. Knapp, L. Lima, D. Werner and E. Bowen, *Environ. Sci. Technol.*, 2011, **45**, 418–424.
3 D. Li and W. Shi, *Chin. J. Catal.*, 2016, **37**, 792–799.
4 X. Bai, W. Chen, B. Wang, T. Sun, B. Wu and Y. Wang, *Int. J. Mol. Sci.*, 2022, **23**, 8130.
5 M. H. Abdurahman, A. Z. Abdullah and N. F. Shoparwe, *Chem. Eng. J.*, 2021, **413**, 127412.
6 (*a*) J. O. Adeyemi, T. Ajiboye and D. C. Onwudiwe, *Water, Air, Soil Pollut.*, 2021, **232**, 219; (*b*) K. Kümmerer, *Chemosphere*, 2019, **75**, 417–434.
7 (*a*) F. Zhao, D. Zhang, C. Y. Xu, J. S. Liu and C. S. Shen, *Ecotoxicol. Environ. Saf.*, 2020, **196**, 110552; (*b*) J. Jeong, W. Song, W. J. Cooper, J. Jung and J. Greaves, *Chemosphere*, 2010, **78**(5), 533–540; (*c*) R. Daghrir and P. Drogui, *Environ. Chem. Lett.*, 2013, **11**(3), 209–227.
8 (*a*) S. M. Marques, E. A. Enyedy, C. T. Supuran, N. I. Krupenko, S. A. Krupenko and M. A. Santos, *Bioorg. Med. Chem.*, 2010, **18**, 5081–5089; (*b*) W. Baran, E. Adamek, J. Ziemianska and A. Sobczak, *J. Hazard. Mater.*, 2011, **196**, 1–15; (*c*) Y. Zhang, J. Xu, Z. Zhong, C. Guo, L. Li, Y. He, W. Fan and Y. Chen, *Environ. Sci. Pollut. Res. Int.*, 2013, **20**(4), 2372–2380.
9 (*a*) N. Casson and G. Greub, *Int. J. Antimicrob. Agents*, 2006, **27**, 541–544; (*b*) M. Feng, Z. Wang, D. D. Dionysiou and V. K. Sharma, *J. Hazard. Mater.*, 2018, **344**, 1136–1154; (*c*) N. Janecko, L. Pokludova, J. Blahova, Z. Svobodova and I. Literak, *Environ. Toxicol. Chem.*, 2016, **35**(11), 2647–2656.
10 (*a*) B. J. Ni, S. T. Zeng, W. Wei, X. H. Dai and J. Sun, *Sci. Total Environ.*, 2020, **703**, 134899; (*b*) C. S. McArdell, E. Molnar, M. J.-F. Suter and W. Giger, *Environ. Sci. Technol.*, 2003, **37**(24), 5479–5486; (*c*) S. Babic, L. Curkovic, D. Ljubas and M. Cizmic, *Curr. Opin. Green Sustainable Chem.*, 2017, **6**, 34–41.
11 (*a*) H. Cho, T. Uehara and T. G. Bernhardt, *Cell*, 2014, **159**, 1300–1311; (*b*) I. Braschi, S. Blasioli, C. Fellet, R. Lorenzini, A. Garelli, M. Pori and D. Giacomini, *Chemosphere*, 2013, **93**(1), 152–159; (*c*) S. Dancer, *J. Antimicrob. Chemother.*, 2001, **48**(4), 463–478; (*d*) P. Ray, K. F. Knowlton, C. Shang and K. Xia, *PLoS One*, 2014, **9**(11), e112343; (*e*) J. Dewdney, L. Maes, J. Raynaud, F. Blanc, J. Scheid, T. Jackson, S. Lens and C. Verschueren, *Food Chem. Toxicol.*, 1991, **29**(7), 477–483; (*f*) R. Gothwal and T. Shashidhar, *Clean: Soil, Air, Water*, 2015, **43**(4), 479–489.
12 (*a*) P. W. Seo, N. A. Khan and S. H. Jhung, *Chem. Eng. J.*, 2017, **315**, 92–100; (*b*) A. Mantovani and A. Macri, *J. Exp. Clin. Cancer Res.*, 2002, **21**(4), 445–456.
13 (*a*) F. Santos-Beneit, M. Ordonez-Robles and J. F. Martin, *Biochem. Pharmacol.*, 2017, **133**, 74–85; (*b*) F. J. Angulo, O. E. Heuer, A. M. Hammerum, P. Collignon and H. C. Wegener, *Clin. Infect. Dis.*, 2006, **43**(7), 911–916.
14 (*a*) D. Sharma, M. Lata, M. Faheem, A. U. Khan, B. Joshi, K. Venkatesan, S. Shukla and D. Bisht, *Microb. Pathog.*, 2019, **132**, 150–155; (*b*) S. Ji, F. Zhang, X. Luo, B. Yang, G. Jin, J. Yan and X. Liang, *J. Chromatogr. A*, 2013, **1313**, 113–118.
15 (*a*) A. Chatzitakis, C. Berberidou, I. Paspaltsis, G. Kyriakou, T. Sklaviadis and I. Poulios, *Water Res.*, 2008, **42**(1–2), 386–394; (*b*) X. Liu, J. C. Steele and X.-Z. Meng, *Environ. Pollut.*, 2017, **223**, 161–169.
16 (*a*) C.-H. Liu, Y.-H. Chuang, H. Li, B. J. Teppen, S. A. Boyd, J. M. Gonzalez, C. T. Johnston, J. Lehmann and W. Zhang, *J. Environ. Qual.*, 2016, **45**(2), 519–527; (*b*) L. Ge, Q. Liu, D. Jiang, L. Ding, Z. Wen, Y. Guo, C. Ding and K. Wang, *Biosens. Bioelectron.*, 2019, **135**, 145–152.
17 K. R. Davies, Y. Cherif, G. P. Pazhani, S. Anantharaj, H. Azzi, C. Terashima, A. Fujishima and S. Pitchaimuthu, *J. Photochem. Photobiol., C*, 2021, **48**, 100437.
18 (*a*) M. B. Ahmed, J. L. Zhou, H. H. Ngo, W. Guo, N. S. Thomaidis and J. Xu, *J. Hazard. Mater.*, 2017, **323**, 274–298; (*b*) S. Li, C. You, K. Rong, C. Zhuang, X. Chen and B. Zhang, *Adv. Powder Mater.*, 2024, **3**, 100183; (*c*) M. Cai, Y. Liu, K. Dong, X. Chen and S. Li, *Chin. J. Catal.*, 2023, **52**, 239–251; (*d*) S. Li, M. Cai, Y. Liu, C. Wang, R. Yan and X. Chen, *Adv. Powder Mater.*, 2023, **2**, 100073; (*e*) A. L. Valenzuela, M. Green and X. Chen, *Gen. Chem.*, 2021, **7**, 210006; (*f*) S. Li, M. Cai, Y. Liu, C. Wang, K. Lv and X. Chen, *Chin. J. Catal.*, 2022, **43**, 2652–2664; (*g*) X. Shen, B. Song, X. Shen, C. Shen, S. Shan, Q. Xueb, X. Chene and S. Li, *Chem. Eng. J.*, 2022, **445**, 136703; (*h*) S. Li, C. You, K. Rong, C. Zhuang, X. Chen and B. Zhang, *Adv. Powder Mater.*, 2024, **3**, 100183; (*i*) S. Li, M. Cai, C. Wang and Y. Liu, *Adv. Fiber Mater.*, 2023, **5**, 994–1007; (*j*) C. Wang, K. Rong, Y. Liu, F. Yang and S. Li, *Sci. China Mater.*, 2024, **67**, 562–572.
19 (*a*) P. P. Singh, S. Sinha, P. Nainwal, P. K. Singh and V. Srivastava, *RSC Adv.*, 2024, **14**, 2590–2601; (*b*) P. P. Singh and V. Srivastava, *ChemistrySelect*, 2023, **8**(44), e202302732; (*c*) V. Srivastava, S. Sinha, D. Kumar and P. P. Singh, *Tetrahedron Green Chem.*, 2023, **1**, 100009; (*d*) P. P. Singh, J. Singh and V. Srivastava, *RSC Adv.*, 2023, **13**, 10958; (*e*) P. P. Singh, P. K. Singh and V. Srivastava, *Org. Chem. Front.*, 2023, **10**, 216; (*f*) P. P. Singh, S. Sinha, G. Pandey and V. Srivastava, *RSC Adv.*, 2022, **12**, 29826; (*g*) V. Srivastava, P. K. Singh and P. P. Singh, *J. Photochem. Photobiol., C*, 2022, **50**, 100488; (*h*) V. Srivastava, P. K. Singh, S. Tivari and P. P. Singh, *Org. Chem. Front.*, 2022, **9**, 1485; (*i*) P. P. Singh, S. Sinha, P. Nainwal, S. Tivari and V. Srivastava, *Org. Biomol. Chem.*, 2024, **22**, 2523–2538.
20 (*a*) S. Tivari, M. Z. Beg, A. Kashyap, P. K. Singh, P. P. Singh, P. Gahtori and V. Srivastava, *Results Chem.*, 2024, **7**, 101249; (*b*) M. Z. Beg, S. Tivari, A. Kashyap, P. K. Singh, P. P. Singh, P. Nainwal and V. Srivastava, *J. Heterocycl. Chem.*, 2024, **61**, 458–465; (*c*) R. Kumar, K. Garima, V. Srivastava, P. P. Singh and P. K. Singh, *Tetrahedron Lett.*, 2023, **133**, 154841; (*d*)

V. P. Singh, A. K. Singh, V. Srivastava and P. P. Singh, *Tetrahedron*, 2023, **147**, 133658; (*e*) M. Mishra, P. P. Singh, P. Nainwal, S. Tivari and V. Srivastava, *Tetrahedron Lett.*, 2023, **129**, 154749; (*f*) V. Srivastava, S. Tivari, P. K. Singh and P. P. Singh, *Catal. Lett.*, 2024, **154**, 771–779; (*g*) M. Z. Beg, P. K. Singh, P. P. Singh, M. Srivastava and V. Srivastava, *Mol. Divers.*, 2024, **28**, 61–71; (*h*) S. P. Singh, V. Srivastava, P. K. Singh and P. P. Singh, *Tetrahedron*, 2023, **132**, 133245; (*i*) M. Mishra, V. Srivastava, P. K. Singh and P. P. Singh, *Croat. Chem. Acta*, 2022, **95**(1), 25–30; (*j*) S. Tivari, P. K. Singh, P. P. Singh and V. Srivastava, *RSC Adv.*, 2022, **12**, 35221.

21 X. Yang, Z. Chen, W. Zhao, C. Liu, X. Qian, M. Zhang, G. Wei, E. Khan, Y. H. Ng and Y. S. Ok, *Chem. Eng. J.*, 2021, **405**, 126806.

22 B. Akyon, M. McLaughlin, F. Hernandez, J. Blotevogel and K. Bibby, *Environ. Sci.: Processes Impacts*, 2019, **21**, 279–290.

23 Z. Cetecioglu and M. Atasoy, *Toxicity and Biodegradation Testing*, 2018, pp. 29–55.

24 (*a*) J. Zhang, H. Lin, J. Ma, W. Sun, Y. Yang and X. Zhang, *Sci. Total Environ.*, 2019, **649**, 396–404; (*b*) C. Zhuang, Y. Chang, W. Li, S. Li, P. Xu, H. Zhang, Y. Zhang, C. Zhang, J. Gao, G. Chen, T. Zhang, Z. Kang and X. Han, *ACS Nano*, 2024, **18**, 5206–5217.

25 L. V. de Souza Santos, A. M. Meireles and L. C. Lange, *J. Environ. Manage.*, 2015, **154**, 8–12.

26 M. S. Yahya, N. Oturan, K. El Kacemi, M. El Karbane, C. Aravindakumar and M. A. Oturan, *Chemosphere*, 2014, **117**, 447–454.

27 V. Homem and L. Santos, *J. Environ. Manage.*, 2011, **92**, 2304–2347.

28 A. Boukhelkhal, O. Benkortbi and M. Hamadache, *Environ. Technol.*, 2018, **40**, 3328–3336.

29 J. Luo, X. Li, C. Ge, K. Müller, H. Yu, P. Huang, J. Li, D. C. W. Tsang, N. S. Bolan, J. Rinklebe and H. Wang, *Bioresour. Technol.*, 2018, **263**, 385–392.

30 J. Wang, Q. Yao, C. Sheng, C. Jin and Q. Sun, *J. Nanomater.*, 2017, **2017**, 1–10.

31 Q. Zhao, S. Zhang, X. Zhang, L. Lei, W. Ma, C. Ma, L. Song, J. Chen, B. Pan and B. Xing, *Environ. Sci. Technol.*, 2017, **51**, 13659–13667.

32 I. A. Lawal and B. Moodley, *J. Chem. Technol. Biotechnol.*, 2017, **92**, 808–818.

33 C. H. Liu, Y. H. Chuang, H. Li, B. J. Teppen, S. A. Boyd, J. M. Gonzalez, C. T. Johnston, J. Lehmann and W. Zhang, *J. Environ. Qual.*, 2016, **45**, 519–527.

34 G. Li, Y. Feng, W. Zhu and X. Zhang, *Korean J. Chem. Eng.*, 2015, **32**, 2109–2115.

35 V. M. Nurchi, M. Crespo-Alonso, M. I. Pilo, N. Spano, G. Sanna and R. Toniolo, *Arabian J. Chem.*, 2019, **12**, 1141–1147.

36 W. C. Li and M. H. Wong, *Int. J. Environ. Sci. Technol.*, 2014, **12**, 2731–2740.

37 A. Zhou, Y. Zhang, R. Li, X. Su and L. Zhang, *Water Treat.*, 2016, **57**, 388.

38 S. Jia, Z. Yang, K. Ren, Z. Tian, C. Dong, R. Ma, G. Yu and W. Yang, *J. Hazard. Mater.*, 2016, **317**, 593–601.

39 O. A. Alsager, M. N. Alnajrani, H. A. Abuelizz and I. A. Aldaghmani, *Ecotoxicol. Environ. Saf.*, 2018, **158**, 114–122.

40 Y. Ji, Z. Pan, D. Yuan and B. Lai, *Clean: Soil, Air, Water*, 2018, **46**, 1700666.

41 R. Kidak and S. Dogan, *Ultrason. Sonochem.*, 2018, **40**, 131–139.

42 M. Feng, L. Yan, X. Zhang, P. Sun, S. Yang, L. Wang and Z. Wang, *Sci. Total Environ.*, 2016, **541**, 167–175.

43 K. S. Tay and N. Madehi, *Sci. Total Environ.*, 2015, **520**, 23–31.

44 R. B. P. Marcelino, M. M. D. Leao, R. M. Lago and C. C. Amorim, *J. Environ. Manage.*, 2017, **195**, 110–116.

45 S. S. M. Hassan, H. I. Abdel-Shafy and M. S. M. Mansour, *Arabian J. Chem.*, 2016, **12**, 4074–4083.

46 B. Kamarehie, F. Ahmadi, F. Hafezi, A. Abbariki, R. Heydari and M. A. Karami, *Data Brief*, 2018, **18**, 96–101.

47 (*a*) P. Karaolia, I. Michael-Kordatou, E. Hapeshi, J. Alexander, T. Schwartz and D. FattaKassinos, *Chem. Eng. J.*, 2017, **310**, 491–502; (*b*) V. Sharma, R. Vinoth Kumar, K. Pakshirajan and G. Pugazhenthi, *Powder Technol.*, 2017, **321**, 259–269; (*c*) J. Zheng, C. Su, J. Zhou, L. Xu, Y. Qian and H. Chen, *Chem. Eng. J.*, 2017, **317**, 309–316; (*d*) M. R. Ramli, N. M. Sulaiman, M. A. Mohd and M. F. Rabuni, *Water Sci. Technol.*, 2015, **72**, 1611–1620.

48 (*a*) S. Chang, X. Yang, Y. Sang and H. Liu, *Chem. Asian J.*, 2016, **11**, 2352–2371; (*b*) U. I. Gaya and A. H. Abdullah, *J. Photochem. Photobiol., C*, 2008, **9**, 1–12; (*c*) J. C. Colmenares and R. Luque, *Chem. Soc. Rev.*, 2014, **43**, 765–778.

49 (*a*) E. S. Elmolla and M. Chaudhuri, *Desalination*, 2010, **252**, 46–52; (*b*) A. C. Nogueira, L. E. Gomes, J. A. P. Ferencz, J. E. F. S. Rodrigues, R. V. Gonçalves and H. Wender, *J. Phys. Chem. C*, 2019, **123**, 25680–25690.

50 (*a*) W. Tu, Y. Zhou and Z. Zou, *Adv. Funct. Mater.*, 2013, **23**, 4996–5008; (*b*) H. L. Tan, F. F. Abdi and Y. H. Ng, *Chem. Soc. Rev.*, 2019, **48**, 1255–1271.

51 A. A. Oladipo and F. S. Mustafa, *Beilstein J. Nanotechnol.*, 2023, **14**, 291–321.

52 X. Bai, W. Chen, B. Wang, T. Sun, B. Wu and Y. Wang, *Int. J. Mol. Sci.*, 2022, **23**, 8130.

53 *Photocatalytic Degradation of Toxic Pesticides*, ed. A. A. Oladipo, M. Gazi, A. O. Ifebajo, A. S. Oladipo and E. O. Ahaka, Wiley, Chicago, 2020, pp. 93–138, DOI: **10.1002/9781119631422.ch4**.

54 *Advanced Oxidation Processes for Waste Water Treatment*, ed. S. C. Ameta and R. Ameta, Elsevier, Academic Press, 2018, DOI: **10.1016/c2016-0-00384-4**.

55 Z. Wei, J. Liu and W. Shangguan, *Chin. J. Catal.*, 2020, **41**, 1440–1450.

56 T. Velempini, E. Prabakaran and K. Pillay, *Mater. Today Chem.*, 2021, **19**, 100380.

57 S. S. Imam, R. Adnan and N. H. M. Kaus, *Toxicol. Environ. Chem.*, 2018, **100**, 518–539.

58 K. Qin, Q. Zhao, H. Yu, X. Xia, J. Li, S. He, L. Wei and T. An, *Environ. Res.*, 2021, **199**, 111360.

59 M. A. Gunawan, J.-C. Hierso, D. Poinsot, A. A. Fokin, N. A. Fokina, B. A. Tkachenko and P. R. Schreiner, *New J. Chem.*, 2014, **38**, 28–41.
60 Y. Li, Y. Fu and M. Zhu, *Appl. Catal., B*, 2020, **260**, 118149.
61 K. Soutsas, V. Karayannis, I. Poulios, A. Riga, K. Ntampegliotis, X. Spiliotis and G. Papapolymerou, *Desalination*, 2010, **250**, 345–350.
62 X. Chen, J. Yao, B. Xia, J. Gan, N. Gao and Z. Zhang, *J. Hazard. Mater.*, 2020, **383**, 121220.
63 M. F. Pinto, M. Olivares, A. Vivancos, G. Guisado-Barrios, M. Albrecht and B. Royo, *Catal. Sci. Technol.*, 2019, **9**, 2421–2425.
64 M. Muruganandham and M. Swaminathan, *Sol. Energy Mater. Sol. Cells*, 2004, **81**, 439–457.
65 A. Taghizadeh, M. Taghizadeh, M. M. Sabzehmeidani, F. Sadeghfar and M. Ghaedi, Chapter 1—Electronic Structure: From Basic Principles to Photocatalysis, in *Interface Science and Technology*, ed. M. Ghaedi, Elsevier, Amsterdam, The Netherlands, 2021, vol. 32, pp. 1–53, ISBN 1573-4285.
66 F. Sadeghfar, Z. Zalipour, M. Taghizadeh, A. Taghizadeh and M. Ghaedi, Chapter 2—Photodegradation Processes, in *Interface Science and Technology*, ed. M. Ghaedi, Elsevier, Amsterdam, The Netherlands, 2021, vol. 32, pp. 55–124, ISBN 1573-4285.
67 O. Sacco, V. Vaiano, C. Han, D. Sannino and D. D. Dionysiou, *Appl. Catal., B*, 2015, **164**, 462–474.
68 G. Zhao, J. Ding, F. Zhou, X. Chen, L. Wei, Q. Gao, K. Wang and Q. Zhao, *Chem. Eng. J.*, 2021, **405**, 126704.
69 E. Topkaya, M. Konyar, H. C. Yatmaz and K. Öztürk, *J. Colloid Interface Sci.*, 2014, **430**, 6–11.
70 M. Ni, M. K. H. Leung, D. Y. C. Leung and K. Sumathy, *Renew. Sustain. Energy Rev.*, 2007, **11**, 401–425.
71 V. Subhiksha, S. Kokilavani and S. S. Khan, *Chemosphere*, 2022, **290**, 133228.
72 F. Zhu, Y. Lv, J. Li, J. Ding, X. Xia, L. Wei, J. Jiang, G. Zhang and Q. Zhao, *Chemosphere*, 2020, **252**, 126577.
73 L. Wang, Z. Wang, L. Zhang and C. Hu, *Chem. Eng. J.*, 2018, **352**, 664–672.
74 M. Batool, M. F. Nazar, A. Awan, M. B. Tahir, A. Rahdar, A. E. Shalan, S. Lanceros-Méndez and M. N. Zafar, *Nano-Struct. Nano-Objects*, 2021, **27**, 100762.
75 (*a*) P. Khanna, A. Kaur and D. Goyal, *J. Microbiol. Methods*, 2019, **163**, 105656; (*b*) N. Baig, I. Kammakakam and W. Falath, *Adv. Mater.*, 2021, **2**, 1821–1871.
76 F. Ahmad, D. Zhu and J. Sun, *Environ. Sci. Eur.*, 2021, **33**, 64.
77 Y. Chen, J. Yang, L. Zeng and M. Zhu, *Crit. Rev. Environ. Sci. Technol.*, 2022, **52**(8), 1401–1448.
78 S. Liu, X.-r. Zhao, H.-y. Sun, R.-p. Li, Y.-f. Fang and Y.-p. Huang, *Chem. Eng. J.*, 2013, **231**, 441–448.
79 F. Guo, W. Shi, H. Wang, M. Han, H. Li, H. Huang, Y. Liu and Z. Kang, *Catal. Sci. Technol.*, 2017, **7**, 3325–3331.
80 D. Qiao, Z. Li, J. Duanb and X. He, *Chem. Eng. J.*, 2020, **400**, 125952.
81 G. Rathee, N. Singh and R. Chandra, *ACS Omega*, 2020, **5**, 2368–2377.
82 Z. Liu, M. Zhu, L. Zhao, C. Deng, J. Ma, Z. Wang, H. Liu and H. Wang, *Chem. Eng. J.*, 2017, **314**, 59–68.
83 J. Yang, Y. Lin, X. Yang, T. B. Ng, X. Ye and J. Lin, *J. Hazard. Mater.*, 2017, **322**, 525–531.
84 N. K. Eswar, S. A. Singh and G. Madras, *Chem. Eng. J.*, 2018, **332**, 757–774.
85 M. H. Khan, H. Bae and J. Y. Jung, *J. Hazard. Mater.*, 2010, **181**, 659–665.
86 Y. Ji, Y. Shi, W. Dong, X. Wen, M. Jiang and J. Lu, *Chem. Eng. J.*, 2016, **298**, 225–233.
87 K. Chakraborty, T. Pal and S. Ghosh, *ACS Appl. Nano Mater.*, 2018, **1**, 3137–3144.
88 Z. Xie, Y. Feng, F. Wang, D. Chen, Q. Zhang, Y. Zeng, W. Lv and G. Liu, *Appl. Catal., B*, 2018, **229**, 96–104.
89 T. Xu, R. Zou, X. Lei, X. Qi, Q. Wu, W. Yao and Q. Xu, *Appl. Catal., B*, 2019, **245**, 662–671.
90 Y. Hong, C. Li, B. Yin, D. Li, Z. Zhang, B. Mao, W. Fan, W. Gu and W. Shi, *Chem. Eng. J.*, 2018, **338**, 137–146.
91 D. Jiang, P. Xiao, L. Shao, D. Li and M. Chen, *Ind. Eng. Chem. Res.*, 2017, **56**(31), 8823–8832.
92 C. Zhou, C. Lai, P. Xu, G. Zeng, D. Huang, Z. Li, C. Zhang, M. Cheng, L. Hu, J. Wan, F. Chen, W. Xiong and R. Deng, *ACS Sustain. Chem. Eng.*, 2018, **6**(5), 6941–6949.
93 Q. Liu, J. Shen, X. Yang, T. Zhang and H. Tang, *Appl. Catal., B*, 2018, **232**, 562–573.
94 M. Yan, Y. Hua, F. Zhu, W. Gu, J. Jiang, H. Shen and W. Shi, *Appl. Catal., B*, 2017, **202**, 518–527.
95 W. Wang, J. Fang, S. Shao, M. Lai and C. Lu, *Appl. Catal., B*, 2017, **217**, 57–64.
96 J. Lyu, J. Shao, Y. Wang, Y. Qiu, J. Li, T. Li, Y. Peng and F. Liu, *Chem. Eng. J.*, 2019, **358**, 614–620.
97 L. Ren, W. Zhou, B. Sun, H. Li, P. Qiao, Y. Xu, J. Wu, K. Lin and H. Fu, *Appl. Catal., B*, 2019, **240**, 319–328.
98 R. Hailili, Z.-Q. Wang, M. Xu, Y. Wang, X.-Q. Gong, T. Xu and C. Wang, *J. Mater. Chem. A*, 2017, **5**(40), 21275–21290.
99 X. Yuan, D. Shen, Q. Zhang, H. Zou, Z. Liu and F. Peng, *Chem. Eng. J.*, 2019, **369**, 292–301.
100 F. Chen, Q. Yang, J. Sun, F. Yao, S. Wang, Y. Wang, X. Wang, X. Li, C. Niu, D. Wang and G. Zeng, *ACS Appl. Mater. Interfaces*, 2016, **8**(48), 32887–32900.
101 T. Wang, W. Quan, D. Jiang, L. Chen, D. Li, S. Meng and M. Chen, *Chem. Eng. J.*, 2016, **300**, 280–290.
102 M. Yan, Y. Wu, F. Zhu, Y. Hua and W. Shi, *Phys. Chem. Chem. Phys.*, 2016, **18**(4), 3308–3315.
103 C. Chen, H. Zeng, M. Yi, G. Xiao, S. Xu, S. Shen and B. Feng, *Appl. Catal., B*, 2019, **252**, 47–54.
104 N. Nasseh, L. Taghavi, B. Barikbin and M. A. Nasseri, *J. Clean. Prod.*, 2018, **179**, 42–54.
105 D. Wang, F. Jia, H. Wang, F. Chen, Y. Fang, W. Dong, G. Zeng, X. Li, Q. Yang and X. Yuan, *J. Colloid Interface Sci.*, 2018, **519**, 273–284.
106 D. B. Hernandez-Uresti, A. Martınez-de la Cruz and L. M. Torres-Martınez, *Ceram. Int.*, 2016, **42**(2), 3096–3103.
107 W. Shi, H. Ren, M. Li, K. Shu, Y. Xu, C. Yan and Y. Tang, *Chem. Eng. J.*, 2020, **382**, 122876.
108 A. O. Oluwole and O. S. Olatunji, *Environ. Sci. Eur.*, 2022, **34**, 5.

109 S. Ghosh, K. Chakraborty, T. Pal and S. Ghosh, *Sci. Rep.*, 2023, **13**, 19028.
110 M. Sharma, M. K. Mandal, S. Pandey, R. Kumar and K. K. Dubey, *ACS Omega*, 2022, **7**, 33572–33586.
111 B. Zhu, Q. Dong, J. Huang, M. Yang, X. Chen, C. Zhai, Q. Chen, B. Wang, H. Tao and L. Chen, *ACS Omega*, 2023, **8**, 13702–13714.
112 Y. M. Hunge, A. A. Yadav, S.-W. Kang and H. Kim, *J. Colloid Interface Sci.*, 2022, **606**, 454–463.
113 S. Li, C. Wang, Y. Liu, M. Cai, Y. Wang, H. Zhang, Y. Guo, W. Zhao, Z. Wang and X. Chen, *Chem. Eng. J.*, 2022, **429**, 132519.
114 L. Biswal, B. P. Mishra, S. Das, L. Acharya, S. Nayak and K. Parida, *Inorg. Chem.*, 2023, **62**, 7584–7597.
115 (*a*) T. B. Nguyen, P. N. T. Ho, C. W. Chen, C. P. Huang, R. Doong and C. D. Dong, *Environ. Sci.: Nano*, 2022, **9**, 229; (*b*) S. Li, C. Wang, Y. Liu, M. Cai, Y. Wang, H. Zhang, Y. Guoc, W. Zhaod, Z. Wange and X. Chen, *Chem. Eng. J.*, 2022, **429**, 132519; (*c*) S. Li, J. Chen, S. Hu, H. Wang, W. Jiang and X. Chen, *Chem. Eng. J.*, 2020, **402**, 126165; (*d*) S. Li, C. Wang, Y. Liu, B. Xue, W. Jiang, Y. Liu, L. Mo and X. Chen, *Chem. Eng. J.*, 2021, **415**, 128991.
116 Q. Chen, S. Wu and Y. Xin, *Chem. Eng. J.*, 2016, **302**, 377–387.
117 W. Zhao, J. Duan, B. Ji, L. Ma and Z. Yang, *J. Environ. Chem. Eng.*, 2020, **8**(1), 102206.
118 N. Shao, J. Wang, D. Wang and P. Corvini, *Appl. Catal., B*, 2017, **203**, 964–978.
119 H. Chen, Y. P. Peng, K. F. Chen, C. H. Lai and Y. C. Lin, *J. Environ. Sci.*, 2016, **44**, 76–87.
120 Y. Yang, G. Zeng, D. Huang, C. Zhang, D. He, C. Zhou, W. Wang, W. Xiong, X. Li, B. Li, W. Dong and Y. Zhou, *Appl. Catal., B*, 2020, **272**, 118970.
121 R. Hassandoost, S. R. Pouran, A. Khataee, Y. Orooji and S. W. Joo, *J. Hazard. Mater.*, 2019, **376**, 200–211.
122 B. Zhou, Y. Li, J. Bai, X. Li, F. Li and L. Liu, *Appl. Surf. Sci.*, 2019, **464**, 115–124.
123 X.-J. Wen, C.-G. Niu, L. Zhang and G.-M. Zeng, *ACS Sustain. Chem. Eng.*, 2017, **5**(6), 5134–5147.
124 Y. Gao, W. Yang, F. Wang, Y. Li, S. Cui, X. Liao and J. Yang, *J. Taiwan Inst. Chem. Eng.*, 2023, **152**, 105160.
125 S. Zhang, S. Zhao, S. Huang, B. Hu, M. Wang, Z. Zhang, L. He and M. Du, *Chem. Eng. J.*, 2021, **420**, 130516.
126 J. Shan, X. Wu, C. Li, J. Hu, Z. Zhang, H. Liu, P. Xia and X. Huang, *Mater. Today Commun.*, 2022, **33**, 104941.
127 J. Mehralipour, S. Darvishali, S. Bagheri and M. Kermani, *Sci. Rep.*, 2023, **13**, 11113.
128 H. Sun, T. Zhou, J. Kang, Y. Zhao, Y. Zhang, T. Wang and X. Yin, *Sep. Purif. Technol.*, 2022, **299**, 121771.
129 J. H. Kim, H. Y. Jang, S. B. Kim, J. W. Choi and J. A. Park, *Water, Air, Soil Pollut.*, 2022, **233**, 480.
130 K. Ouyang, C. Yang, B. Xu, H. Wang and S. Xie, *Colloids Surf., A*, 2021, **625**, 126978.
131 J. Y. Chin, A. L. Ahmad and S. C. Low, *J. Environ. Manage.*, 2023, **343**, 118231.
132 Y. Li, S. Wang, H. Guo, J. Zhou, Y. Liu, T. Wang and X. Yin, *Chemosphere*, 2024, **352**, 141371.
133 J. Gao, Y. Gao, Z. Sui, Z. Dong, S. Wang and D. Zou, *J. Alloys Compd.*, 2018, **732**, 43–51.
134 X.-J. Wen, C.-H. Shen, C.-G. Niu, D.-C. Lai, M.-S. Zhu, J. Sun, Y. Hu and Z.-H. Fei, *J. Mol. Liq.*, 2019, **288**, 111063.
135 W. Liu, Z. Li, Q. Kang and L. Wen, *Environ. Res.*, 2021, **197**, 110925.
136 F. Berdini, J. O. Otalvaro, M. Avena and M. Brigante, *Results Eng.*, 2022, **16**, 100765.
137 W. Liu, J. Zhang, J. Jia and C. Yuan, *Powder Technol.*, 2024, **433**, 119201.
138 K. Wang, X. Yu, F. Yang, Z. Liu, T. Zhang, J. Niu and B. Yao, *Adv. Powder Technol.*, 2023, **34**, 104157.
139 Y. Zhao, Y. Wang, E. Liu, J. Fan and X. Hu, *Appl. Surf. Sci.*, 2018, **436**, 854–864.
140 C.-c. Hao, F.-y. Chen, K. Bian, Y.-b. Tang and W.-l. Shi, *Beilstein J. Nanotechnol.*, 2022, **13**, 1038–1050.
141 W. Baran, E. Adamek, J. Ziemianska and A. Sobczak, *J. Hazard. Mater.*, 2011, **196**, 1–15.
142 Q. Dinh, E. Moreau-Guigon, P. Labadie, F. Alliot, M. J. Teil, M. Blanchard, J. Eurin and M. Chevreuil, *Sci. Total Environ.*, 2017, **575**, 758–766.
143 R. Yin, W. Guo, N. Ren, L. Zeng and M. Zhu, *Water Res.*, 2020, **171**, 115374.
144 W. Yan, L. Yan and C. Jing, *Appl. Catal., B*, 2019, **244**, 475–485.
145 T.-B. Nguyen, C. Huang, R.-a. Doong, C.-W. Chen and C.-D. Dong, *Chem. Eng. J.*, 2020, **384**, 123383.
146 M. Chen, C. Guo, S. Hou, L. Wu, J. Lv, C. Hu, Y. Zhang and J. Xu, *J. Hazard. Mater.*, 2019, **366**, 219–228.
147 M. Ren, Y. Ao, P. Wang and C. Wang, *Chem. Eng. J.*, 2019, **378**, 122122.
148 W. Zhu, F. Sun, R. Goei and Y. Zhou, *Appl. Catal., B*, 2017, **207**, 93–102.
149 S. Naraginti, Y.-Y. Yu, Z. Fang and Y.-C. Yong, *Chem. Eng. J.*, 2019, **375**, 122035.
150 P. Karaolia, I. Michael-Kordatou, E. Hapeshi, C. Drosou, Y. Bertakis, D. Christofilos, G. S. Armatas, L. Sygellou, T. Schwartz, N. P. Xekoukoulotakis and D. Fatta-Kassinos, *Appl. Catal., B*, 2018, **224**, 810–824.
151 H. Zhang, Z. Wang, R. Li, J. Guo, Y. Li, J. Zhu and X. Xie, *Chemosphere*, 2017, **185**, 351–360.
152 E. Ioannidou, Z. Frontistis, M. Antonopoulou, D. Venieri, I. Konstantinou, D. I. Kondarides and D. Mantzavinos, *Chem. Eng. J.*, 2017, **318**, 143–152.
153 M. Jahdi, S. B. Mishra, E. N. Nxumalo, S. D. Mhlanga and A. K. Mishra, *Appl. Catal., B*, 2020, **267**, 118716.
154 J. Yang, Z. Li and H. Zhu, *Appl. Catal., B*, 2017, **217**, 603–614.
155 A. Mirzaei, L. Yerushalmi, Z. Chen, F. Haghighat and J. Guo, *Water Res.*, 2018, **132**, 241–251.
156 A. Yazdanbakhsh, A. Eslami, M. Massoudinejad and M. Avazpour, *Chem. Eng. J.*, 2020, **380**, 122497.
157 O. Mertah, A. Gómez-Avilés, A. Slassi, A. Kherbeche, C. Belver and J. Bedia, *Catal. Commun.*, 2023, **157**, 106611.
158 X. Gan, Y. Song, G. Liu, H. Zhang and J. Yang, *Front. Environ. Sci.*, 2023, **11**, 1314536.
159 J. Musial, D. T. Mlynarczyk and B. J. Stanisz, *Sci. Total Environ.*, 2023, **856**, 159122.

160 J. Dang, W. Pei, F. Hu, Z. Yu, S. Zhao, J. Hu, J. Liu, D. Zhang, Z. Jing and X. Lei, *Toxics*, 2023, **11**(10), 818.
161 X. Lin, H. Fang, L. Wang, D. Sun, G. Zhao and J. Xu, *Water*, 2024, **16**, 218.
162 J. Zhang, S. Gou, Z. Yang, C. Li and W. Wang, *Water Cycle*, 2024, **5**, 1–8.
163 D. Yongheng, Y. Huayu, L. Jiang, S. Qia, Y. Qianwena and Z. Yuntao, *RSC Adv.*, 2023, **13**, 5957–5969.
164 J.-Y. Zhang, J. Ding, L.-M. Liu, R. Wu, L. Ding, J.-Q. Jiang, J.-W. Pang, Y. Li, N.-Q. Ren and S.-S. Yang, *Environ. Sci. Ecotechnology*, 2024, **17**, 100308.
165 N. Le-Duy, L.-A. T. Hoang, T. D. Nguyen and T. Lee, *Chemosphere*, 2023, **321**, 138118.
166 A. A. Ioannidi, J. Zappa, A. Petala, M. Souliotis, D. Mantzavinos and Z. Frontistis, *Water*, 2023, **15**(7), 1370.
167 L. Pan, C. Jiao, Y. Liang, J. Xiong, S. Wang, H. Zhu, G. Chenc and H. Song, *New J. Chem.*, 2021, **45**, 5645–5653.
168 A. Adewuyi, O. A. Ogunkunlec and R. A. Oderinde, *RSC Adv.*, 2023, **13**, 9563–9575.
169 Y. Fang, H. Chen, T. Sheng, S. Lv, S. Cai, Y. Liu and K. Zhang, *Surface. Interfac.*, 2024, **45**, 103848.
170 H. Chen, Y. Fang, P. Duan, X. Zhang and K. Zhang, *ChemistrySelect*, 2023, **8**, e202300658.
171 N. Le-Duy, L.-A. T. Hoang, T. D. Nguyen and T. Lee, *ACS Appl. Nano Mater.*, 2023, **6**(16), 14798–14809.
172 P. Wang, X. Gu, S. Li, J. Shen, J. Liu, C. Gong and Y. Chen, *Environ. Technol.*, 2023, 1–16.
173 V. K. Parida, S. K. Srivastava, S. Chowdhury and A. K. Gupta, *Langmuir*, 2023, **39**(51), 18846–18865.
174 X. Liu, J. Xu, T. Zhang, J. Zhang, D. Xia, Y. Du, Y. Jiang and K. Lin, *J. Colloid Interface Sci.*, 2023, **629**, 989–1002.
175 B. Zhang, C. Fang, J. Ning, R. Dai, Y. Liu, Q. Wu, F. Zhang, W. Zhang, S. Dou and X. Liu, *Carbon Neutralization*, 2023, **2**, 646–660.
176 C.-S. Lu, H.-Y. Tsai, J. Shaya, V. B. Golovko, S.-Y. Wang, W.-J. Liug and C.-C. Chen, *RSC Adv.*, 2022, **12**, 29709–29718.
177 N. Roy, K. Kannabiran and A. Mukherjee, *Chemosphere*, 2023, **333**, 138912.
178 Y. Li, W. Zhu, Q. Guo, X. Wang, L. Zhang, X. Gao and Y. Luo, *Sep. Purif. Technol.*, 2021, **276**, 119403.
179 B. Yang, X. Mao, L. Pi, Y. Wu, H. Ding and W. Zhang, *Environ. Sci. Pollut. Res. Int.*, 2017, **24**(9), 8658–8670.
180 C. Zhou, P. Xu, C. Lai, C. Zhang, G. Zeng, D. Huang, M. Cheng, L. Hu, W. Xiong, X. Wen, L. Qin, J. Yuan and W. Wang, *Chem. Eng. J.*, 2019, **359**, 186–196.
181 C. Zhou, Z. Zeng, G. Zeng, D. Huang, R. Xiao, M. Cheng, C. Zhang, W. Xiong, C. Lai, Y. Yang, W. Wang, H. Yi and B. Li, *J. Hazard. Mater.*, 2019, **380**, 120815.
182 C. Zhou, C. Lai, D. Huang, G. Zeng, C. Zhang, M. Cheng, L. Hu, J. Wan, W. Xiong, M. Wen, X. Wen and L. Qin, *Appl. Catal., B*, 2018, **220**, 202–210.
183 H. Ji, P. Du, D. Zhao, S. Li, F. Sun, E. C. Duin and W. Liu, *Appl. Catal., B*, 2020, **263**, 118357.
184 T.-W. Tzeng, S.-L. Wang, C.-C. Chen, C.-C. Tan, Y.-T. Liu, T.-Y. Chen, Y.-M. Tzou, C. C. Chen and J. T. Hung, *RSC Adv.*, 2016, **6**(73), 69301–69310.
185 X.-J. Wen, X.-X. Lv, J. Sun, J. Guo, Z.-H. Fei and C.-G. Niu, *J. Hazard. Mater.*, 2020, **385**, 121508.
186 S. Dong, X. Ding, T. Guo, X. Yue, X. Han and J. Sun, *Chem. Eng. J.*, 2017, **316**, 778–789.
187 S. Dong, L. Cui, C. Liu, F. Zhang, K. Li, L. Xia, X. Su, J. Feng, Y. Zhu and J. Sun, *J. Taiwan Inst. Chem. Eng.*, 2019, **97**, 288–296.
188 M.-A. Edaala, L. E. Mersly, A. A. Tahiri, P. Wong-Wah-Chung, L. E. Blidi, M. M. Alrashed and S. Rafqah, *Water*, 2023, **15**(23), 4058.
189 X. Zeng, S. Shu, Y. Meng, H. Wang and Y. Wang, *Chem. Eng. J.*, 2023, **456**, 141105.
190 S. Shu, H. Wang, X. Guo, Y. Wang and X. Zeng, *Sep. Purif. Technol.*, 2023, **323**, 124458.
191 D. Liang, Z. Lin, Y. Wu, D. Li, J. Chen, X. Jin, Y. Chen, J. Zhang, H. Liu, P. Chen, W. Lv and G. Liu, *Environ. Sci.: Nano*, 2023, **10**, 1053–1064.
192 Y. M. Bakier and H. M. El-Bery, *J. Environ. Chem. Eng.*, 2023, **11**, 111493.
193 W. Zhu, J. Liu, S. Yu, Y. Zhou and X. Yan, *J. Hazard. Mater.*, 2016, **318**, 407–416.
194 R. Wang, J. Tang, X. Zhang, D. Wang, X. Wang, S. Xue, Z. Zhang and D. D. Dionysiou, *J. Hazard. Mater.*, 2019, **375**, 161–173.
195 Y. Wu, H. Ji, Q. Liu, Z. Sun, P. Li, P. Ding, M. Guo, X. Yi, W. Xu, C.-C. Wang, S. Gao, Q. Wang, W. Liu and S. Chen, *J. Hazard. Mater.*, 2022, **424**, 127563.
196 Q. Li, Z. Guan, D. Wu, X. Zhao, S. Bao, B. Tian and J. Zhang, *ACS Sustain. Chem. Eng.*, 2017, **5**(8), 6958–6968.
197 X. Xu, L. Meng, Y. Dai, M. Zhang, C. Sun, S. Yang, H. He, S. Wang and H. Li, *J. Hazard. Mater.*, 2020, **381**, 120953.
198 M. Liu, D. Zhang, J. Han, C. Liu, Y. Ding, Z. Wang and A. Wang, *Chem. Eng. J.*, 2020, **382**, 123017.
199 X. Xin, H. Liu, J. Sun, K. Gao and R. Jia, *Int. J. Environ. Sci. Technol.*, 2023, **20**, 11865–11876.
200 N. Wang, X. Li, Y. Yang, Z. Zhou, Y. Shang and X. Zhuang, *J. Water Process Eng.*, 2020, **36**, 101335.
201 X. Liu, Y. Liu, S. Lu, W. Guo and B. Xi, *Chem. Eng. J.*, 2018, **350**, 131–147.
202 D. Li, N. Zhang, R. Yuan, H. Chen, F. Wang and B. Zhou, *J. Environ. Chem. Eng.*, 2021, **9**, 106243.
203 Q. Li, H. Y. Yang, P. Z. Zhong, N. J. Jiancong, W. Yang, J. Chen, Y. Zhang and L. Jianmin, *Sep. Purif. Technol.*, 2022, **299**, 121814.
204 C. P. Silva, D. Pereira, V. Calisto, M. A. Martins, M. Otero, V. Esteves and D. L. D. Lima, *J. Environ. Manag.*, 2021, **294**, 112937.
205 W. Yang, C. Bu, M. Zhao, Y. Li, S. Cui, J. Yang and H. Lian, *Small*, 2024, 2309972.
206 M. Feng, Z. Wang, D. D. Dionysiou and V. K. Sharma, *J. Hazard. Mater.*, 2018, **344**, 1136–1154.
207 D. M. Whitacre, *Reviews of Environmental Contamination and Toxicology*, Springer, 2009, vol. 217.
208 N. Janecko, L. Pokludova, J. Blahova, Z. Svobodova and I. Literak, *Environ. Toxicol. Chem.*, 2016, **35**(11), 2647–2656.
209 X. Van Doorslaer, J. Dewulf, H. Van Langenhove and K. Demeestere, *Sci. Total Environ.*, 2014, **500–501**, 250–269.

210 M. Feng, Z. Wang, D. D. Dionysiou and V. K. Sharma, *J. Hazard. Mater.*, 2018, **344**, 1136–1154.
211 M. Golmohammadi, H. Hanafi-Bojd and M. Shiva, *Ceram. Int.*, 2023, **49**, 7717–7726.
212 I. Mukherjee, V. Cilamkoti and R. K. Dutta, *ACS Appl. Nano Mater.*, 2021, **4**(8), 7686–7697.
213 R. Noroozi, M. Gholami, V. Oskoei, M. H. Arani, S. A. Mousavifard, B. N. Le and M. Fattahi, *Sci. Rep.*, 2023, **13**, 16287.
214 H. Alshaikh, A. Shawky, R. M. Mohamed, J. K. Knight and L. S. Roselin, *J. Mol. Liq.*, 2021, **334**, 116092.
215 M. Manasa, P. R. Chandewar and H. Mahalingam, *Catal. Today*, 2021, **375**(375), 522–536.
216 N. Moghni, H. Boutoumi, H. Khalaf, N. Makaoui and G. Colon, *J. Photochem. Photobiol., A*, 2022, **428**, 113848.
217 C. Gherasim, P. Pascariu, M. Asandulesa, M. Dobromir, F. Doroftei, N. Fifere, A. Dascalu and A. Airinei, *Ceram. Int.*, 2022, **48**, 25556–25568.
218 C. H. Shen, X. J. Wen, Z. H. Fei, Z. T. Liu and Q. M. Mu, *Chem. Eng. J.*, 2020, **391**, 123612.
219 S. A. Abdulrahman, Z. Y. Shnain, S. S. Ibrahim and H. S. Majdi, *Catalysts*, 2022, **12**, 1663.
220 P. Pascariu, C. Cojocaru, M. Homocianu, P. Samoila, A. Dascalu and M. Suchea, *Ceram. Int.*, 2022, **48**, 4953–4964.
221 P. Pascariu, C. Cojocaru, M. Homocianu and P. Samoila, *J. Environ. Manag.*, 2022, **316**, 115317.
222 P. Pascariu, C. Cojocaru, P. Samoila and C. Romanitan, *Int. J. Mol. Sci.*, 2023, **24**, 6436.
223 B. Zhu, D. Song, T. Jia, W. Sun, D. Wang, L. Wang, J. Guo, L. Jin, L. Zhang and H. Tao, *ACS Omega*, 2021, **6**(2), 1647–1656.
224 T. J. Al-Musawi, N. Mengelizadeh, A. I. Alwared, D. Balarak and R. Sabaghi, *Environ. Sci. Pollut. Res.*, 2023, **30**, 70076–70093.
225 J. Zuo, X. Ma, C. Tan, Z. Xia, Y. Zhang, S. Yu, Y. Li, Yu. Li and J. Li, *Anal. Methods*, 2023, **15**, 519–528.
226 L. Wolski, K. Grzelak, M. Muńko, M. Frankowski, T. Grzyb and G. Nowaczyk, *Appl. Surf. Sci.*, 2021, **563**, 150338.
227 Z. Nasari and M. Taherimehr, *Langmuir*, 2023, **39**(40), 14357–14373.
228 N. Kumar, R. Gusain, M. Masukume and S. S. Ray, *Sol. RRL*, 2023, **7**, 2300475.
229 M. Xu, Y. Wang, E. Ha, H. Zhang and C. Li, *Chemosphere*, 2021, **265**, 129013.
230 Y. Zhao, Y. Zuo, G. He, Q. Chen, Q. Meng and H. Chen, *J. Alloys Compd.*, 2021, **869**, 159305.
231 Z. Chen, J. Liang, X. Xu, G. He and H. Chen, *J. Mater. Sci.*, 2020, **55**, 6065.
232 J. V. Kumar, R. Karthik, S.-M. Chen, V. Muthuraj and C. Karuppiah, *Sci. Rep.*, 2016, **6**, 34149.
233 H. Zhu, B. Yang, J. Yang, Y. Yuan and J. Zhang, *Chemosphere*, 2021, **276**, 130217.
234 M. Manjunatha and H. Mahalingam, *Sci. Rep.*, 2013, **13**, 14631.
235 S. Kaushal, V. Kumari and P. P. Singh, *Environ. Sci. Pollut. Res.*, 2023, **30**, 65602–65617.
236 A. R. Dash, A. J. Lakhani, D. D. Priya, T. V. Surendra, M. M. R. Khan, E. J. J. Samuel and S. M. Roopan, *J. Cluster Sci.*, 2023, **34**, 121–133.
237 N. A. A. M. Azan, S. Sagadevan, A. R. Mohamed, A. H. N. Azazi, F. B. M. Suah, T. Kobayashi, R. Adnan and N. H. M. Kaus, *Catalysts*, 2020, **12**(10), 1269.
238 P. Rajiv, N. Mengelizadeh, G. McKay and D. Balarak, *Int. J. Environ. Anal. Chem.*, 2023, **103**, 2193–2207.
239 H. Qin, Y. Yang, W. Shia and Y. She, *RSC Adv.*, 2021, **11**, 13731–13738.
240 H. Zhang, Z. Fan, Q. Chai and J. Li, *Catalysts*, 2023, **13**(3), 469.
241 S. Uruş, M. Çaylar, H. Eskalen and Ş. Özgan, *J. Mater. Sci.: Mater. Electron.*, 2022, **33**, 4314–4329.
242 Y. Peng, J. Lin, J.-L. Niu, X. Guo, Y. Chen, T. Hu, J. Cheng and Y. Hu, *ACS Appl. Mater. Interfaces*, 2024, **16**(2), 2351–2364.
243 M. Murugalakshmi, K. Govindan, M. Umadevi, C. B. Breslin and V. Muthuraj, *Environ. Sci.: Water Res. Technol.*, 2023, **9**, 1385–1402.
244 C. Chuaicham, T. Inoue, V. Balakumar, Q. Tian, B. Ohtani and K. Sasaki, *J. Environ. Chem. Eng.*, 2022, **10**, 106970.
245 H. Qin, Y. Yang, W. Shia and Y. She, *RSC Adv.*, 2021, **11**, 13731–13738.
246 J. Cheng, Z. Deng, X. Zheng, C. Chu and Y. Guo, *J. Alloys Compd.*, 2024, **971**, 172779.
247 S. G. Khasevani, D. Nikjoo, C. Chaxel, K. Umeki, S. Sarmad, J.-P. Mikkola and I. Concina, *ACS Omega*, 2023, **8**(46), 44044–44056.
248 Z. Jia, T. Li, Z. Zheng, J. Zhang, J. Liu, R. Li, Y. Wang, X. Zhang, Y. Wang and C. Fan, *Chem. Eng. J.*, 2020, **380**, 122422.
249 S. Wu, Y. Su, Y. Zhu, Y. Zhang and M. Zhu, *Appl. Surf. Sci.*, 2020, **520**, 146339.
250 Y. Li, Y. Fu and M. Zhu, *Appl. Catal., B*, 2020, **260**, 118149.
251 S. Dong, L. Cui, W. Zhang, L. Xia, S. Zhou, C. K. Russell, M. Fan, J. Feng and J. Sun, *Chem. Eng. J.*, 2020, **384**, 123279.
252 S. Dong, L. Cui, Y. Tian, L. Xia, Y. Wu, J. Yu, D. M. Bagley, J. Sun and M. Fan, *J. Hazard. Mater.*, 2020, **399**, 123017.
253 S. L. Prabavathi, K. Saravanakumar, C. M. Park and V. Muthuraj, *Sep. Purif. Technol.*, 2021, **257**, 117985.
254 A. Machín, L. Soto-Vázquez, D. García, M. C. Cotto, D. Ortiz, P. J. Berríos-Rolón, K. Fontánez, E. Resto, C. Morant, F. Petrescu and F. Márquez, *Catalysts*, 2023, **13**(3), 538.
255 H. Qi, M. Wu, J. Wang, B. Zhang, C. Dai, F. Teng, M. Zhao and L. He, *ChemistrySelect*, 2023, **8**, e202204121.
256 X. Zhong, K.-X. Zhang, D. Wu, X.-Y. Ye, W. Huang and B.-X. Zhou, *Chem. Eng. J.*, 2020, **383**, 123148.
257 L. Wen, P. Liu, Z. Zhou, K. Wang and Y. Zhou, *Chem.–Asian J.*, 2023, **18**, e202300161.
258 B. Trifi, A. Nahdi, A. Othmani, Z. Aloui, M. Essid and H. Dhaouadi, *Int. J. Environ. Sci. Technol.*, 2024, **21**, 3747–3760.
259 J. Li, Z. Yin, J. Guo, W. Gan, R. Chen, M. Zhang and Z. Sun, *RSC Adv.*, 2024, **14**, 4975–4989.
260 C.-K. Tsai, Y.-C. Lee, T. T. Nguyen and J.-J. Horng, *Chemosphere*, 2022, **298**, 134285.

261 H. Wei, F. Meng, W. Yu, J. Li and H. Zhang, *Sep. Purif. Technol.*, 2023, **318**, 123940.
262 L. Zhang, L. Tan, Z. Yuan, B. Xu, W. Chen, Y. Tang, L. Li and J. Wang, *Chem. Eng. J.*, 2023, **452**, 139327.
263 Q. Su, J. Li, H. Yuan, B. Wang, Y. Wang, Y. Li and Y. Xing, *Chem. Eng. J.*, 2022, **427**, 131594.
264 Q. Shang, X. Liu, M. Zhang, P. Zhang, Y. Ling, G. Cui, W. Liu, X. Shi, J. Yue and B. Tang, *Chem. Eng. J.*, 2022, **443**, 136354.
265 G. Gupta, S. K. Kansal, A. Umar and S. Akbar, *Chemosphere*, 2023, **314**, 137611.
266 M. Malhotra, A. Garg and M. Rawat, *Chem. Eng. Technol.*, 2024, **47**, 683–691.
267 Z. Xiao, J. Xiao, L. Yuan, M. Ai, F. Idrees, Z.-F. Huang, C. Shi, X. Zhang, L. Pan and J.-J. Zou, *J. Mater. Chem. A*, 2024, **12**, 5366–5376.
268 L. Shi, X. Zou, T. Wang, D. Wang, M. Fan and Z. Gong, *Chin. Chem. Lett.*, 2022, **33**, 442–446.
269 B. Wang, K. Qian, W. Yang, W. An, L.-L. Lou, S. Liu and K. Yu, *Front. Chem. Sci. Eng.*, 2023, **17**, 1728–1740.
270 H. Yin, H. Shi, L. Sun, D. Xia and X. Yuan, *Environ. Sci. Pollut. Res.*, 2021, **28**, 11650–11664.
271 X. Liu, Y. Zhong, H. Feng, Y. Zhao, Q. Li and T. Huang, *New J. Chem.*, 2024, **48**, 800–810.
272 Z. Shan, F. Ma, M. Xu, X. Shan, L. Shan, Ch. Cui and H. Guo, *Chem. Eng. J.*, 2023, **466**, 143229.
273 J. Xu, Z. Ren, X. Qiu, P. Zhu, D. Chen, L. Xie and C. Zhang, *ChemistrySelect*, 2021, **6**, 7295–7305.
274 X. Liu, Y. Zhong, H. Feng, Y. Zhao, Q. Li and T. Huang, *New J. Chem.*, 2024, **48**, 800–810.
275 A. A. Mashentseva, D. T. Nurpeisova and M. Barsbay, *RSC Adv.*, 2024, **14**, 4424–4435.
276 Q. Chen, Y. H. Z. Song, M. Liu, D. Chen, B. Zhu, J. Chen and Z. Chen, *Ecotoxicol. Environ. Saf.*, 2021, **225**, 112742.
277 S. Kar, T. Pal and S. Ghosh, *ACS Appl. Nano Mater.*, 2024, **7**, 6516–6524.
278 S. Kar, T. Pal and S. Ghosh, *ChemistrySelect*, 2023, **8**, e202300878.
279 H. Cai, Y. Ma, J. Li, Y. Jin, P. Zhu and M. Chen, *Ind. Eng. Chem. Res.*, 2022, **61**(30), 11237–11248.
280 M. Passi and B. Pal, *Chem. Eng. J.*, 2024, **479**, 147685.
281 C. Feng, Y. Wang, Z. Lu, Q. Liang, Y. Zhang, Z. Li and S. Xu, *Sep. Purif. Technol.*, 2022, **282**, 120107.
282 (*a*) W. Zhang, Z. Huang, L. Zhang, Y. Meng, Z. Ni, H. Tang and S. Xia, *J. Environ. Chem. Eng.*, 2023, **11**, 109979; (*b*) S. Li, K. Dong, M. Cai, X. Li and X. Chen, *eScience*, 2024, **4**, 100208.
283 H. Guo, J. Cui, X. Chai, Y. Shi, S. Gao and J. Gao, *Environ. Sci. Pollut. Res.*, 2023, **30**, 68403–68416.
284 K. Wang, S. Zhan, D. Zhang, H. Sun, X. Jina and J. Wang, *RSC Adv.*, 2021, **11**, 4723–4739.
285 T. Li, J. Liu, F. Shi, H. Zhang, H. Zhang, C. Ma and M. Wasim, *J. Environ. Chem. Eng.*, 2023, **11**, 109301.
286 Z. Gong, J. Xie, J. Liu, T. Liu, J. Chen, J. Li and J. Gan, *Environ. Sci. Pollut. Res.*, 2023, **30**, 38700–38712.
287 H. Rahmani, A. R. Mahjoub and Z. Khazaee, *ACS Appl. Nano Mater.*, 2023, **6**(6), 4554–4566.
288 P. Zhou, Y. Wang, L. Jing, X. Yan, Y. Gan, C. Xia, M. Xie and Y. Xu, *Colloids Surf., A*, 2024, **686**, 133380.
289 J. Huang, D. Li, R. Li, P. Chen, Q. Zhang, H. Liu, W. Lv, G. Liu and Y. Feng, *J. Hazard. Mater.*, 2020, **386**, 121634.
290 (*a*) Y. Xiao, H. Lyu, J. Tang, K. Wang and H. Sun, *Chem. Eng. J.*, 2020, **384**, 123311; (*b*) S. Li, C. Wang, K. Dong, P. Zhang, X. Chen and X. Li, *Chin. J. Catal.*, 2023, **51**, 101–112.
291 V. Homem and L. Santos, *J. Environ. Manage.*, 2011, **92**(10), 2304–2347.
292 C. S. McArdell, E. Molnar, M. J.-F. Suter and W. Giger, *Environ. Sci. Technol.*, 2003, **37**(24), 5479–5486.
293 S. M. Mitchell, J. L. Ullman, A. L. Teel and R. J. Watts, *Chemosphere*, 2015, **134**, 504–511.
294 C.-H. Huang, J. E. Renew, K. L. Smeby, K. Pinkston and D. L. Sedlak, *J. Contemp. Water Res. Educ.*, 2011, **120**, 4.
295 C. Guo and P. Li, *Environ. Monit. Assess.*, 2023, **195**, 1423.
296 P. Zhao, Y. Yang, Y. Pei and X. Luo, *Cellulose*, 2023, **30**, 1133–1147.
297 A. Ounnar, A. Bouzaza, L. Favier and F. Bentahar, *Rev. Energ. Renouv.*, 2017, **20**, 683–691.
298 H. Dong, X. Guo, C. Yang and Z. Ouyang, *Appl. Catal., B*, 2018, **230**, 65–76.
299 G. Li, R. Wang, B. Wang and J. Zhang, *Appl. Surf. Sci.*, 2020, **517**, 146212.
300 G. Li, B. Wang, J. Zhang, R. Wang and H. Liu, *Chem. Eng. J.*, 2019, **391**, 123500.
301 H. Dong, X. Guo and Y. Yin, *Res. Chem. Intermed.*, 2018, **44**(5), 3151–3167.
302 L. L. Albornoz, S. W. da Silva, J. P. Bortolozzi, E. D. Banús, P. Brussino, M. A. Ulla and A. M. Bernardes, *Chemosphere*, 2021, **268**, 128858.
303 M. Mohsin, I. A. Bhatti, M. Iqbal, S. Naz, A. Ashar, J. Nisar, F. F. Al-Fawzan and S. A. Alissa, *J. Water Proc. Eng.*, 2021, **44**, 102433.
304 P. Karaolia, I. Michael-Kordatou, E. Hapeshi, C. Drosou, Y. Bertakis, D. Christofilos, G. S. Armatas, L. Sygellou, T. Schwartz, N. P. Xekoukoulotakis and D. Fatta-Kassinos, *Appl. Catal., B*, 2018, **224**, 810–824.
305 N. P. Xekoukoulotakis, N. Xinidis, M. Chroni, D. Mantzavinos, D. Venieri, E. Hapeshi and D. Fatta-Kassinos, *Catal. Today*, 2010, **151**(1–2), 29–33.
306 G. Li, B. Wang, J. Zhang, R. Wang and H. Liu, *Appl. Surf. Sci.*, 2019, **478**, 1056–1064.
307 B. Gao, S. Dong, J. Liu, L. Liu, Q. Feng, N. Tan, T. Liu, L. Bo and L. Wang, *Chem. Eng. J.*, 2016, **304**, 826–840.
308 R. Hendili, A. Alatrache, M. Ben-Attia and M.-N. Pons, *C. R. Chim.*, 2017, **20**(7), 710–716.
309 D. Tassalit, N. Chekir, O. Benhabiles, F. Bentahar and N. A. Laoufi, *Green Energy and Technology*, Springer, Cham, 2016, pp. 695–706. DOI: **10.1007/978-3-319-30127-3_51**.
310 V. Vaiano, O. Sacco, D. Sannino and P. Ciambelli, *Chem. Eng. J.*, 2015, **261**, 3–8.
311 L. Chen, W. Ma, J. Dai, J. Zhao, C. Li and Y. Yan, *J. Photochem. Photobiol., A*, 2016, **328**, 24–32.
312 P. Karaolia, I. Michael-Kordatou, E. Hapeshi, C. Drosou, Y. Bertakis, D. Christofilos, G. S. Armatas, L. Sygellou,

T. Schwartz, N. P. Xekoukoulotakis and D. Fatta-Kassinos, *Appl. Catal., B*, 2018, **224**, 810–824.
313 S. Naraginti, Y.-Y. Yu, Z. Fang and Y.-C. Yong, *Process Saf. Environ. Prot.*, 2019, **125**, 39–49.
314 M. H. Sayadi, S. Sobhani and H. Shekari, *J. Clean. Prod.*, 2019, **232**, 127–136.
315 G.-I. Lupu, C. Orbeci, C. Bobirică, L. Bobirică, E. S. Lazăr, J. Pandele-Cusu, M. N. Verziu, C. Pîrvu and R.-G. Irodia, *Sustainable Environ. Res.*, 2023, **33**, 36.
316 A. Mehrdoost, R. J. Yengejeh, M. K. Mohammadi, A. Haghighatzadeh and A. A. Babaei, *Environ. Sci. Pollut. Res.*, 2022, **29**, 33514–33527.
317 B. Loder, G. Newton and E. Abraham, *Biochem. J.*, 1961, **79**, 408–416.
318 Y. Wang, R. L. Tennyson and D. Romo, *Heterocycles*, 2004, **64**, 605–658.
319 V. Vaiano, O. Sacco, D. Sannino and P. Ciambelli, *Chem. Eng. J.*, 2015, **261**, 3–8.
320 S. Fallahizadeh, M. Gholami, M. R. Rahimi, A. Esrafili, M. Farzadkia and M. Kermani, *Sci. Rep.*, 2023, **13**, 16185.
321 R. M. B. Ramos, L. C. Paludo, P. I. Monteiro, L. V. M. da Rocha, C. V. de Moraes, O. O. Santos, E. R. Alves and T. L. P. Dantas, *Talanta*, 2023, **260**, 124658.
322 E. T. Wahyuni, R. N. Cahyono, M. Nora, E. Z. Alharissa and E. S. Kunarti, *Results Chem.*, 2024, **7**, 101302.
323 F. Beshkar, A. Al-Nayili, O. Amiri, M. Salavati-Niasari and M. Mousavi-Kamazani, *J. Alloys Compd.*, 2022, **892**, 162176.
324 D. Balarak, N. Mengelizadeh, P. Rajiv and K. Chandrika, *Environ. Sci. Pollut. Res.*, 2011, **28**, 49743–49754.
325 I. F. Silva, I. F. Teixeira, R. D. F. Rios, G. M. do Nascimento, I. Binatti, H. F. V. Victória, K. Krambrock, L. A. Cury, A. P. C. Teixeira and H. O. Stumpf, *J. Hazard. Mater.*, 2021, **401**, 123713.
326 N. Zulfiqar, R. Nadeem and O. A. Musaimi, *ACS Omega*, 2024, **9**(7), 7986–8004.
327 Z.-H. Diao, J.-C. Jin, M.-Y. Zou, H. Liu, J.-Q. Qin, X.-H. Zhou, W. Qian, P.-R. Guo, L.-J. Kong and W. Chu, *Sep. Purif. Technol.*, 2021, **278**, 119620.
328 G. Rana, P. Dhiman, J. Sharma, A. Kumar and G. Sharma, *Inorg. Chem. Commun.*, 2023, **158**, 111596.
329 P. Debnath, K. Sen, A. Mondal, A. Mondal and N. K. Mondal, *Int. J. Environ. Res.*, 2021, **15**, 571–583.
330 F. M. d. Rosa, J. Papac, S. Garcia-Ballesteros, M. Kovačić, Z. Katančić, H. Kušić and A. L. Božić, *Adv. Sustainable Syst.*, 2021, **5**, 2100119.
331 A. Fawzy, H. Mahanna and M. Mossad, *Environ. Sci. Pollut. Res.*, 2022, **29**, 68532–68546.
332 Y. T. Gaim, S. M. Yimanuh, Z. G. Kidanu and J. Compos, *Science*, 2022, **6**(10), 317.
333 T. T. Nguyen, S.-N. Nam, J. Son and J. Oh, *Sci. Rep.*, 2019, **9**, 9349.
334 M. Verma and A. K. Haritash, *Environ. Technol. Innovation*, 2020, **20**, 101072.
335 T. D. N. Thi, L. H. Nguyen, X. H. Nguyen, H. V. Phung, T. H. T. Vinh, P. V. Viet, N. V. Thai, H. N. Le, D. T. Pham, H. T. Van, L. H. T. Thi, T. D. P. Thi, T. L. Minh, H. H. P. Quang, H. P. N. Vu, T. T. Duc and H. M. Nguyen, *Mater. Sci. Semicond. Process.*, 2022, **142**, 106456.
336 M. Dou, J. Wang, B. Gao, C. Xu and F. Yang, *Chem. Eng. J.*, 2020, **383**, 123134.
337 B. Gao, J. Wang, M. Dou, C. Xu and X. Huang, *Environ. Sci. Pollut. Res.*, 2020, **27**(7), 7025–7039.
338 M. Chahkandi and M. Zargazi, *J. Hazard. Mater.*, 2020, **389**, 121850.
339 S. Le, W. Yang, G. Chen, A. Yan and X. Wang, *Environ. Pollut.*, 2020, **263**, 114550.
340 M.-M. Fang, J.-X. Shao, X.-G. Huang, J.-Y. Wang and W. Chen, *J. Mater. Sci. Technol.*, 2020, **56**, 133–142.
341 N. Pugazhenthiran, P. Sathishkumar, O. Albormani, S. Murugesan, M. Kandasamy, M. Selvaraj, S. Suresh, S. K. Kumar, D. Contreras, H. Váldes and R. V. Mangalaraja, *Chemosphere*, 2023, **313**, 137515.
342 N. Pugazhenthiran, S. Murugesan, H. Valdés, M. Selvaraj, P. Sathishkumar, P. G. Smirniotis, S. Anandan and R. V. Mangalaraja, *J. Ind. Eng. Chem.*, 2022, **105**, 384–392.
343 K. Portillo-Cortez, J. E. Romero-Ibarra, D. Dominguez, G. Alonso-Nuñez and U. Caudillo-Flores, *J. Photochem. Photobiol., A*, 2023, **445**, 115090.
344 J. Yang, L. Fang, Z. Li, G. Meng, Y. Jia, Y. Jiang, J. Lian and X. Gan, *Chemosphere*, 2023, **314**, 137618.
345 N. AttariKhasraghi, K. Zare, A. Mehrizad, N. Modirshahla and M. A. Behnajady, *J. Inorg. Organomet. Polym.*, 2021, **31**, 3164–3174.
346 M. Zhou, L. Cheng, Z. Chen, L. Chen and Y. Ma, *J. Alloys Compd.*, 2021, **869**, 159322.
347 J. He, Y. Zhang, Y. Guo, G. Rhodes, J. Yeom, H. Li and W. Zhang, *Environ. Int.*, 2019, **132**, 105105.
348 A. Almasi, R. Esmaeilpoor, H. Hoseini, V. Abtin and M. Mohammadi, *J. Environ. Health Sci. Eng.*, 2020, **18**, 1359–1373.
349 N. S. Nguyen, T. D. Pham, H. T. Vo and K. D. Ngo, *Environ. Technol.*, 2019, **42**(8), 1292–1301.
350 S. Wang, J. Liu, I. Albaijan, A. Shawabkeh, H. Lin, I. Ahmad, S. O. Rab and M. Y. Alshahrani, *J. Ind. Eng. Chem.*, 2024, **135**, 213–231.
351 A. Bendesky, D. Menendez and P. Ostrosky-Wegman, *Mutat. Res. Rev. Mutat. Res.*, 2022, **511**(2), 133–144.
352 S. Dong, J. Sun, Y. Li, C. Yu, Y. Li and J. Sun, *Appl. Catal., B*, 2014, **144**, 386–393.
353 J. Li, W. Zhao, Y. Guo, Z. Wei, M. Han, H. He, S. Yang and C. Sun, *Appl. Surf. Sci.*, 2015, **351**, 270–279.
354 M. Malakootian, N. Olama, M. Malakootian and A. Nasiri, *Int. J. Environ. Sci. Technol.*, 2019, **16**(8), 4275–4284.
355 F. S. Mustafa and A. A. Oladipo, *J. Water Proc. Eng.*, 2021, **42**, 102132.
356 M. S. H. Shuvo, R. A. Putul, K. S. Hossain, S. M. Masum and M. A. I. Molla, *Toxics*, 2024, **12**(1), 36.
357 Y. Zhang and W. Chu, *Sep. Purif. Technol.*, 2022, **291**, 120900.
358 T. J. Al-Musawi, N. S. M. Moghaddam, S. M. Rahimi, M. Amarzadeh and N. Nasseh, *J. Environ. Manage.*, 2022, **319**, 115697.

359 M. Yeganeh, H. R. Sobhi and A. Esrafili, *Environ. Sci. Pollut. Res.*, 2022, **29**, 25486–25495.
360 Y.-L. Wang, A. Gómez-Avilés, S. Zhang, J. J. Rodriguez, J. Bedia and C. Belver, *J. Environ. Chem. Eng.*, 2023, **11**, 109744.
361 A. Seidmohammadi, Y. Vaziri, A. Dargahi and H. Z. Nasab, *Biomass Conv. Bioref.*, 2023, **13**, 9057–9073.
362 Z. M. Niaki, M. Ghorbani and S. A. Ghoreishi, *J. Environ. Health Sci. Eng.*, 2021, **19**, 1583–1596.
363 H. Cai, D. Zhang, X. Ma and Z. Ma, *Sep. Purif. Technol.*, 2022, **288**, 120633.
364 V. Balakumar, K. Sekar, C. Chuaicham, R. Manivannan and K. Sasaki, *Environ. Sci.: Nano*, 2021, **8**, 2261–2276.
365 A. Kubiak, *Sci. Rep.*, 2023, **13**, 12075.
366 G. S. Sales, A. A. C. França, J. F. Cruz-Filho, C. A. F. Moraes, A. R. S. Neto, A. G. C. Sales, R. S. Santos and G. E. Luz Jr, *J. Environ. Chem. Eng.*, 2023, **11**, 110335.
367 F. Ghribi, M. Sehailia, L. Aoudjit, F. Touahra, D. Zioui, A. Boumechhour, D. Halliche, K. Bachari and Z. Benmaamar, *J. Photochem. Photobiol., A*, 2020, **397**, 112510.
368 B. Farahani, M. Giahi, M. H. Ghorbani, R. Fazaeli and O. Moradi, *J. Nanostruct. Chem.*, 2023, **13**, 303–320.
369 H. Pasdar, N. E. Fard and M. Rezvani, *Appl. Phys. A*, 2023, **129**, 380.
370 R. Sheikhsamany, H. Faghihian and R. Fazaeli, *Mater. Sci. Semicond. Process.*, 2022, **138**, 106310.
371 B. Kakavandi, E. Dehghanifard, P. Gholami, M. Noorisepehr and B. MirzaHedayat, *Appl. Surf. Sci.*, 2021, **570**, 151145.
372 S. Akter, M. S. Islam, M. H. Kabir, M. A. A. Shaikh and M. A. Gafur, *Arabian J. Chem.*, 2022, **15**, 103900.
373 F. S. Arghavan, T. J. Al-Musawi, G. A. Rumman, R. Pelalak, A. Khataee and N. Nasseh, *J. Environ. Chem. Eng.*, 2021, **9**, 105619.
374 S. Fakhravar, M. Farhadian and S. Tangestaninejad, *J. Environ. Chem. Eng.*, 2020, **8**, 104136.
375 S. Sohani, B. Ara, H. Khan, K. Gul and M. Khan, *Environ. Res.*, 2022, **215**, 114262.
376 Z. Li, S. Yuan, Z. Zhang, S. Liu, H. Guo, X. Qi, Z. Wu and J. Guo, *Mater. Res. Bull.*, 2024, **175**, 112755.
377 S. R. Mishra, V. Gadore and M. Ahmaruzzaman, *J. Clean. Prod.*, 2023, **427**, 139221.
378 W. Ahmad, A. Singh, K. K. Jaiswal and P. Gupta, *J. Inorg. Organomet. Polym.*, 2021, **31**, 614–623.
379 J. Zhao, B. Yao, Q. He and T. Zhang, *J. Hazard. Mater.*, 2012, **229–230**, 51–158.
380 L. N. Skvortsova, K. I. Kazantseva, K. A. Bolgaru, A. A. Reger, I. A. Artyukh and K. A. Dychko, *Inorg. Mater.*, 2023, **59**, 321–328.
381 K. Leeladevi, J. Vinoth Kumar, M. Arunpandian, M. Thiruppathi and E. R. Nagarajan, *Mater. Sci. Semicond. Process.*, 2021, **123**, 105563.
382 Z. Zhu, F. Guo, A. Li, W. Xu and X. Zhang, *J. Environ. Sci.*, 2023, **134**, 65–76.
383 C. Zhu, J. Li, Y. Chai, Y. Zhang, Y. Li, X. Zhang, J. Liu and Y. Li, *Front. Chem.*, 2022, **10**, 964008.
384 C.-W. Chien, N. Dhenadhayalan and K.-C. Lin, *J. Environ. Chem. Eng.*, 2023, **11**, 110613.
385 T. L. Palma, B. Vieira, J. Nunes, J. P. Lourenço, O. C. Monteiro and M. C. Costa, *J. Iran. Chem. Soc.*, 2020, **17**, 2013–2031.
386 K. O. Sodeinde, S. O. Olusanya, O. S. Lawal, M. Sriariyanun and A. A. Adediran, *Sci. Rep.*, 2022, **12**, 17054.
387 H. Singh, A. Ahlawat, T. K. Dhiman and P. R. Solanki, *Mater. Lett.*, 2023, **346**, 134504.
388 M. Baneshi, S. Jahanbin, A. Mousavizadeh, S. Sadat, A. Rayegan-Shirazi and H. Biglari, *Pol. J. Environ. Stud.*, 2018, **27**(4), 1433–1439.
389 Y. Deng, J. Liu, Y. Huang, M. Ma, K. Liu, X. Dou, Z. Wang, S. Qu and Z. Wang, *Adv. Funct. Mater.*, 2020, **30**, 2002353.
390 T. Do, D. Q. Nguyen, K. T. Nguyen and P. H. Le, *Materials*, 2019, **12**(15), 2434.
391 F. Dehghani, S. Yousefinejad, M. Dehghani, S. M. Borghei and A. H. Javid, *Int. J. Environ. Sci. Technol.*, 2022, **19**, 8957–8968.
392 F. Dehghani, S. Yousefinejad, M. Dehghani, S. M. Borghei and A. H. Javid, *Int. J. Environ. Anal. Chem.*, 2022, 1–9.